STATE RESEARCH CENTER OF RUSSIA

INSTITUTE FOR HIGH ENERGY PHYSICS

NuMI–B–501

May 31, 1999

Comparison of Initial Conceptual Designs of the Low Energy Target

(Task C Report of the Accord between FNAL and IHEP)

P.Galkin, N.Galyaev, V.Garkusha, V.Gres,
A.Kharlamov, V.Ferapontov, E.Lomakin, A.Ryabov,
F.Novoskoltsev, V.Zarucheisky

Protvino 1999

Contents

1 Introduction

The PH2 focusing system with two parabolic shaped horns has been developed to provide in three steps (1–6 GeV, 2–12 GeV and 5–25 GeV) a wide band neutrino beam for the MINOS experiment. Corresponding low energy (LE), medium energy (ME) and high energy (HE) configurations of this neutrino beam optics design use the same horns and power supply system, but with different targets and different positions of the second horn [1, 2]. The advanced conceptual design of the water cooled fin target for ME and HE beam configurations is given in the previous IHEP Report [3]. This Report gives description of initial conceptual designs of the LE target, i.e. the target for the LE configuration of the PH2 focusing system.

Results of the optimization show that, in order to obtain the most possible number of 1–6 GeV neutrinos in the far MINOS detector, the LE target should be located inside the upstream part of the first Horn, as it is shown in Figure 1.1. Figure 1.2 shows the energy spectra of ν_μ charged current events in the far detector calculated for $R = 2.0$ mm graphite and $R = 3.2$ mm beryllium rod targets. For the NuMI primary proton beam with $\sigma \sim R/2.25$, these values of the target radii are the minimal possible which provide acceptable levels of stresses in target materials [4]. The length of both targets is 0.94 m, it corresponds approximately to 2 and 2.2 of nuclear interaction lengths for graphite and beryllium respectively. Results of these beam simulations (which were made by the GNuMI without any details of the LE target design) show, that both considering target materials [1] give nearly the same neutrino event rate in the far detector.

The possible designs of a target for the LE beam are defined by:

- the way of target cooling (forced water or gas convection), and
- the shape of a target core (cylindrical or fin).

Because the LE target is located inside the Horn 1, the maximum transversal size of a target design is limited by the internal diameter of the horn inner conductor at the downstream end of a target, i.e. it should be less than 40 mm. In this case most of secondaries, contributing to the

[1] Graphite ZXF–5Q of Poco Graphite, Inc. and beryllium S–65C of Brush Wellman, Inc.. have been considered as possible materials for a target core in described below LE target designs. The main properties of these materials are given in [3].

neutrino event rate in the detector, will cross through a whole thickness of the target design, which should be thin enough to minimize the absorption.

Figure 1.3 gives total event rates in the far detector calculated as functions of target sizes for two neutrino energy ranges of the LE beam. All plots are thus normalized that 1.0 is the total event rate in the corresponding energy range for the graphite rod target with the radius of 2.0 mm. As it follows from these plots:

- the equivalent thickness (radius) of a matter in a transversal direction for rod targets should not exceed 6.0–6.5 mm for both graphite and beryllium. The reasonable value of the target core radius is equal to 3.2 mm, because it corresponds to the inventory size of Poco Graphite, Inc. for graphite rods. The rest part of the matter includes target casing and a cooling system;
- similar to rod targets, 3.2 mm for graphite and 4.1 mm for beryllium are optimal thicknesses for fin targets. Besides of the proton beam size in the vertical direction, the fin height of 32 mm also includes target casing and a cooling system.

These limitations in transversal sizes of the target unit were taken into account when considering various conceptual designs of the LE target.

Distributions of the energy deposition density in the target core, as well as those of thermal stresses are in strong dependence on transversal distributions of the proton beam. For all possible designs the beam distributions were calculated using the following procedure:

- The phase space distribution of the proton beam (x,x',y,y',p; total number of particles is equal to 100000) at the input of the electrostatic septum was used by the TURTLE code for simulation of beam parameters in the target.
- Strengths of last five quadrupoles (Q6÷Q10) of the proton beamline [5] were calculated using the TRANSPORT code in order to obtain the necessary proton beam spot size.
- The maximum value of the beam size on the target was limited by the value of $\sigma = 2$ mm, when taking into account innermost radii of both horns and collimators of the baffle protection system.

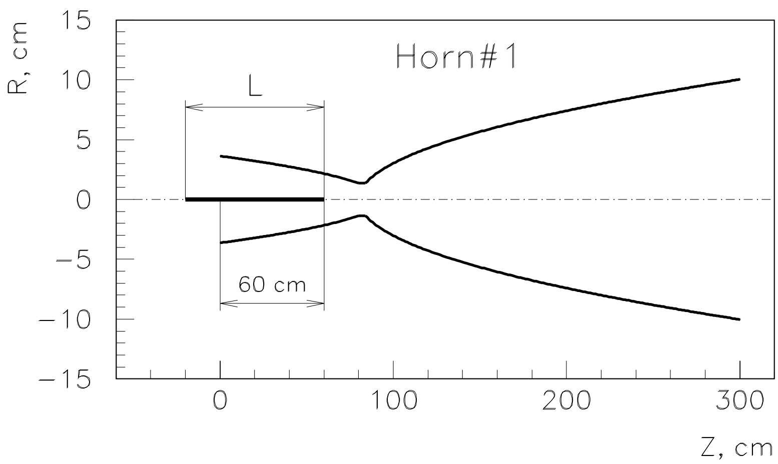

Figure 1.1: The location of the LE target with respect to the Horn 1.

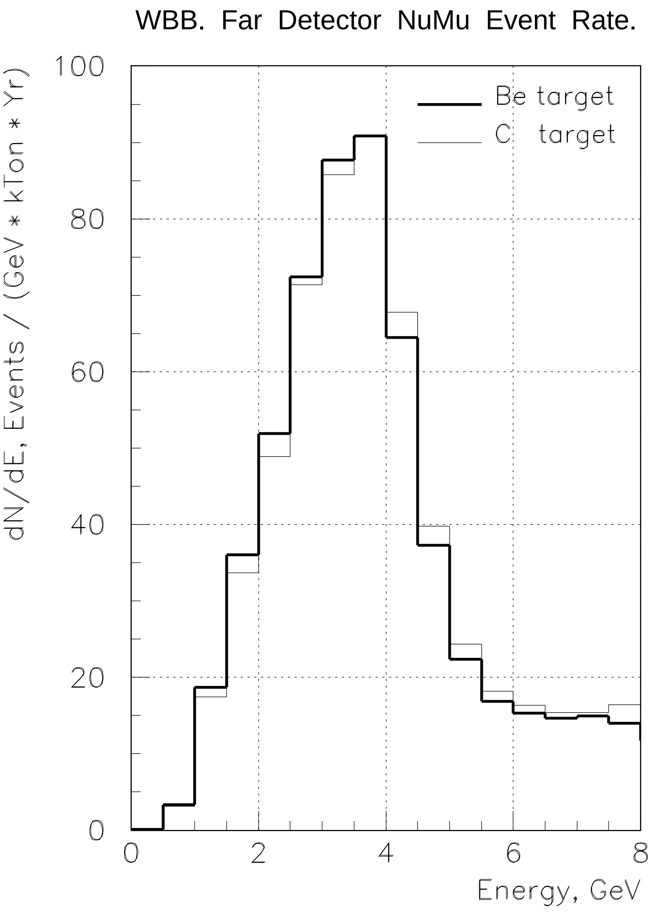

Figure 1.2: Energy spectra of ν_μ CC events in the far MINOS detector for the LE configuration of the PH2 focusing system.

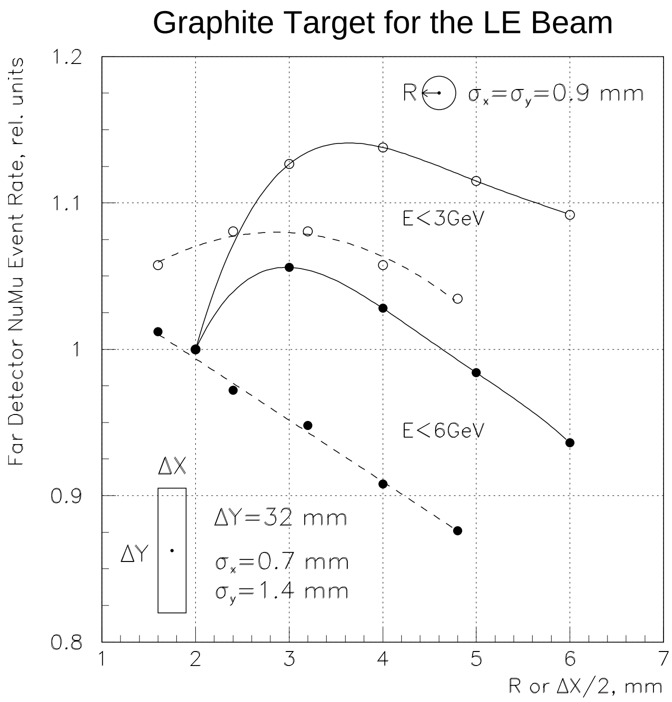

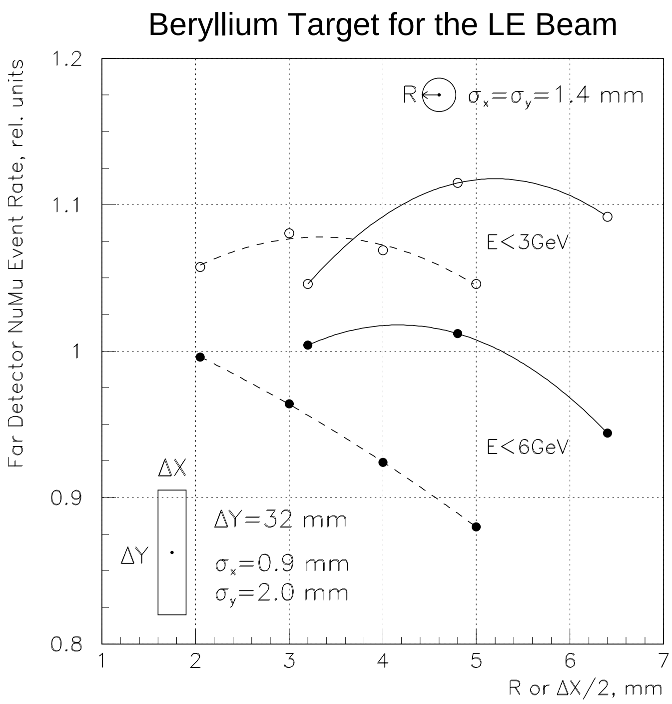

Figure 1.3: Total neutrino events rates in the far detector as functions of transversal sizes for the rod (solid line) and fin (dashed line) LE targets with $L = 0.94$ m. σ_x and σ_y give the proton beam spot size constant for all values of R or $\Delta X/2$ for rod and fin targets respectively.

2 LE Targets with Cylindrical Core

The beam spot sizes for the case of cylindrical target core were chosen $\sigma_x = \sigma_y = 0.89$ mm for graphite and $\sigma_x = \sigma_y = 1.4$ mm for beryllium. The real proton beam distribution was symmetrized by azimuthal averaging in order to use simple formulas for stresses in a heated axial–symmetrically rod. The energy deposition in a target was computed by MARS [6] for the base line intensity equal to $4{\cdot}10^{13}$ protons/spill.

2.1 Energy Deposition in the Target Rod. Stress calculations

The average density of an energy deposition in the 10 cm length target rod as a function of the radius is shown in Figure 2.1. Using a distribution of an energy deposition density one can calculate temperature distribution $T(r)$ taking into account the temperature dependence of a specific heat of target materials:

$$\int_{T_0}^{T} C(T)\, dT = \frac{E(r)}{\rho},$$

where $E(r)$ is the density of an energy deposition, T_0 is the ambient temperature, ρ is the density of the target material and $C(T)$ is its specific heat. The maximum temperature rise is equal to 345°C in graphite and 79°C in beryllium.

The distributions of stresses in a target rod heated by the proton beam in the case of free ends may be defined by formulas [7], modified for the dependence of material properties on the temperature:

$$S_{rr}(r) = \frac{E}{1-\nu}\left[F(r_0) - F(r)\right],$$

$$S_{\varphi\varphi}(r) = \frac{E}{1-\nu}\left[F(r_0) + F(r) - \overline{\alpha}(T)\, T\right],$$

$$S_{zz}(r) = \frac{E}{1-\nu}\left[2F(r_0) - \overline{\alpha}(T)\, T\right],$$

where E is the modulus of an elasticity, $\overline{\alpha}(T(r))$ is an average coefficient of a thermal expansion in a temperature range (T_0, T), ν is the Poisson ratio, r_0 is the target radius and

$$F(r) = \frac{1}{r^2}\int_0^r \overline{\alpha}(T)\, T\, r\, dr.$$

The radial distributions of stresses for graphite and beryllium targets are shown in Figures 2.2. The target core is compressed in radial direction ($S_{rr} \leq 0$) while in longitudinal and azimuthal directions it may be compressed as well as stretched. The equivalent stress reaches its maximum value equal to 22 MPa at $r = 0$ in the graphite target and 95 MPa at $r = r_0$ in beryllium one.

HAST [8] calculations show that given above formulas describe well the stresses only in a central part of the target rod and do not take into account the stress concentration at the end of the rod. The behaviour of equivalent stresses as a function of radius of rounding is given in Figure 2.3 for graphite and beryllium targets. As it follows from these plots, the radius of rounding equal to core radius is quite enough to avoid the stress concentration at the target ends.

2.2 Target with Water Cooling

In the case of forced water cooling the direct contact between water and a target surface cannot be allowed for both types of target materials: graphite and beryllium. For this reason the target core should be encapsulated in a pipe (aluminum or stainless steel) having a good radiation hardness in a high radiation environment. A good thermal contact between target core and external pipe is provided by a shrinkage of the external pipe.

2.2.1 Encapsulating of the Target Core

One of possible ways to get a necessary shrinkage is a shrinking of pipe with the zone-normalized deformation method. The core rods are located in this case inside of a metal pipe with a small gap equal to 0.05–0.1 mm. External pipe is stretched in the longitudinal direction and heated locally by electron beam to the temperature exceeded the elastic limit. In order to have uniform azimuthal heating, the pipe is rotated around its axis. The heating unit (electron beam gun) is moved along the pipe axis with velocity sufficient to heat a pipe to the temperature which exceed the elastic limit. At the initial stage of cooling the external pipe shrinks plastically. When the temperature drops to 500–600°C the pipe shrinks elastically. The resulting value of a prestress can be defined by the following expression:

$$P_0 \simeq (\alpha_m - \alpha_t) E_m \Delta T \, a / r_0,$$

where α_t is the coefficient of a thermal expansion of a target material, α_m is the coefficient of a thermal expansion of a metal pipe, E_m is the modulus of an elasticity of a metal pipe and $\Delta T \simeq 500$–$600°$C is the temperature inelastic limit, a is the thickness of a metal pipe, r_0 is the target radius. For the graphite core and stainless steel 16X12M2C2 (Russian grade widely used in nuclear reactors) $E_m \simeq 200$ GPa, $\alpha_m - \alpha_t = 3 \cdot 10^{-6}$ K^{-1} and at the thickness of an external pipe $a = 0.2$ mm, the prestress $P_0 \simeq 18$ MPa.

The maximum equivalent stress in a target as a function of the prestress value is shown in Figure 2.4 for graphite and beryllium targets. As it follows from this Figure, the maximum equivalent stress in the graphite target core drops at first and reaches its minimum value at $P_0 \simeq 5$ MPa. To provide such small prestress it is necessary to find the grade of a stainless steel having the coefficient of a thermal expansion closed to graphite.

From Russian grades of stainless steels the grade 2X17H1 [9] is the most suitable because its coefficient of a thermal expansion is equal to $8.1 \cdot 10^{-6}$ K^{-1} which is greater than that for graphite ($7.7 \cdot 10^{-6}$ K^{-1}) and the difference of these coefficients is small enough to have prestress value close to its optimum. The estimation for this steel grade by given above formula gives $P_0 \simeq 3$ MPa. This value is rather close to an optimum prestress.

For the target with beryllium core the maximum equivalent stress increases by the value $\sim 0.5 P_0$ (see Figure 2.4). There are a lot of grades of steels with the coefficient of a thermal expansion greater than that for beryllium. At the same time the differences between coefficients are rather small [9].

2.2.2 Target Design

One of possible designs of the LE target with water cooling using the conception of shrinking pipe is shown in Figure 2.5. The target core consists of six 6.4 mm in diameter and 15 cm length graphite or beryllium rods which are encapsulated into the 0.2 mm thick stainless steel pipe. In order to provide a better thermal contact, the target rod may be previously coated by a thin (2–3 microns) copper layer. Two beryllium windows seal and separate the target core in a dry helium environment. Helium is supplied through the 1 mm in diameter pipe. Because the target, as well as the beam has slope with respect to the horizon, helium should be supplied from the downstream end of the pipe.

Cooling water passes from the upstream end to the downstream one inside of water channel formed by two coaxial pipes. The gap between these pipes is equal to 1 mm. Cooling water outlet is made of stainless steel tube of 4 mm in diameter and 0.2 mm wall thickness. The thickness of the external pipe is chosen to 0.3 mm. Such design corresponds to an equivalent thickness of graphite and beryllium equal to 5.2 mm in radius (see Figure 1.3).

Another possible design is shown in Figure 2.6, where outlet water channel is coaxial with input water channel. This design is more complicated in manufacturing and has larger equivalent thickness of the target (~6.2 mm) and consequently lower luminosity (see Figure 1.3).

One of a serious problem of a cylindrical target design is the sag due to its own weight. Some ways of a sag compensation will be discussed below.

2.2.3 Target Cooling

The power depositions along the target in terms of an average power are shown in Figure 2.7. Total power is equal to 2.8 kW for graphite target and 2.15 kW for beryllium one. Such difference of the average power may be explained by the difference in a beam spot sizes for graphite and beryllium at the same target radius.

The heat transfer coefficient to water α_w is defined [10] as

$$\alpha_w = \frac{Nu}{d_h}\lambda,$$

where Nu is the Nusselet number, d_h is the hydraulic diameter of water channel and λ is the heat conductivity of water. Hydraulic diameter of a coaxial cooling channel is equal to $d_2 - d_1$, where d_2, d_1 are the external and internal diameters of a channel. Nusselet number depends on Reynolds Re and Prandtle Pr numbers and for Reynolds numbers in a range of $4 \cdot 10^3 \leq Re \leq 5 \cdot 10^5$ can be calculated by the semiempirical formula [10]:

$$Nu = (\xi/8)\frac{Re\cdot Pr}{1.07 + 900/Re + 12.7(\xi/8)^{0.5}(Pr^{2/3} - 1)},$$

where $\xi = (1.82\lg(Re) - 1.64)^{-2}$.

At the water velocity equal to 3 m/s, sizes of water channel $d_2 = 8.8$ mm and $d_1 = 6.8$ mm Reynolds number $Re = 6 \cdot 10^3$ and $\alpha_w = 17$ kW/m^2/K.

As a result, water temperature rise is equal to 9.0°C for the graphite target and 7.0°C for beryllium one at a total water flow rate equal to 4.4 l/min and a pressure drop along the length of a cooling channel ~0.98 atm. Estimations of a temperature jump at the steel pipe with the heat conductivity $\lambda_m = 10\,\mathrm{W/m/K}$ give 3°C for graphite target and 2.3°C for beryllium one.

2.3 Target with Gas Cooling

Helium was successfully used for cooling of the beryllium target at the CERN neutrino beam for NOMAD and CHORUS [11]. Each of eleven target rods was cooled by the pair of helium jets (the total number is equal to 22 parallel jets). The flow was maximal in the second rod (about 50 l/s), and decreased progressively to the last one (about 10 l/s). The helium flow was provided by a 1465 turns/min Roots pump, delivering 555 l/s at atmospheric pressure to the target box through two water cooled exchangers. The heat transfer coefficient between a target rod and helium was calibrated experimentally and was equal to ~500 W/m^2/K for the first rod.

2.3.1 Target Cooling

Because the LE target design for the NuMI has no space to arrange separate cooling of target rods, there is only one way for the gas cooling: cooling of target rods in series. In this case gas flow propagates longitudinally with respect to the rod axis.

For a forced gas convection a heat transfer coefficient between the target rod and gas does not exceed 100–200 W/m^2/K (air or nitrogen [10]) and 300–500 W/m^2/K (helium [11]). For the target diameter equal to 6.4 mm and deposited average power ~3 kW, power flux through the lateral surface of the target rod is equal to $1.5{\cdot}10^5$ W/m^2. It corresponds to the 1500–750°C (air or nitrogen) and 500–300°C (helium) temperature difference between the cooling gas and target rod. For comparison, in the CERN target the average deposited power is equal to 640 W and at the target length equal to 1.1 m and its diameter equal to 3 mm the power flux is equal to $0.6{\cdot}10^5$ W/m^2, i.e. 2.5 times less than that for the NuMI target. The temperature rise of a cooling gas as a function of its total flow rate is given in Table 2.1.

Temperature rise, °C	10	20	50	100	200
Helium flow rate, l/s	340	170	68	34	17
Nitrogen flow rate, l/s	260	130	52	26	13

Table 2.1: Temperature rise of a cooling gas for different total flow rates.

As it was mentioned above, the diameter of target casing is limited by ∼40 mm. The total flow rate through the cross-section of target casing equal to ∼13 l/s corresponds to the flow velocity equal to ∼10 m/s. In a real design, taking into account the size of the outlet gas channel and cross section area of the target itself, the total gas flow rate should be decreased 3–4 times with respect to this estimated value. But even for the maximum of the cross section area the average target temperature will be of 500–700°C in the case of helium cooling. Using of nitrogen as a cooling gas is practically impossible due to significantly higher temperature of the target.

In order to decrease the average temperature of the target at a limited value of a heat transfer coefficient $\alpha \leq 500$ W/m^2/K, it is necessary to decrease the value of a power flux. It can be achieved by increasing of an area of heat exchanging between the cooling gas and target rod. For this purpose the eight ribs (each 1.3 mm thick and height h) radiator is applied (Figure 2.8). The average temperature, calculated taking into account the radiation with coefficient of an emissivity equal to 0.9 for graphite and 0.7 for beryllium, as a function of a rib height h and heat transfer coefficients are shown in Figure 2.9. One can see that acceptable temperatures of the target rod can be achieved even in the case of nitrogen or air used as a cooling gas ($\alpha = 200$ W/m^2/K) at the rib height of 7–10 mm.

The heat transfer coefficient α_g between the cooling gas and target rod can be calculated via Nusselet (Nu) number, a heat conductivity λ_g of a cooling gas and a characteristic size d_{eq} by the formula given above. The characteristic size d_{eq} for the height of a rib equal to 10 mm may be estimated as 6–8 mm that approximately corresponds to the target rod diameter or to the hydraulic diameter of a cooling channel formed by two neighbour ribs.

Nusselet number is defined via Reynolds (Re) and Prandtle (Pr) numbers by the semiempirical formula:

$$Nu = C Re^m Pr^n,$$

where C, m, n are the correlation coefficients. The values of these coefficients are given in [12] for the case of transversal gas cooling in the range of gas velocities 4–20 m/s: $C = 0.59$, $m = 0.47$, $n = 0.33$.

For a jet directed at the angle ϕ, the value of a heat transfer coefficient should be decreased by $k = 1 - 0.54\cos^2\phi$. In the case of longitudinal jet $\phi = 90°$ and $k = 0.46$. On the other hand, the given above formula for Nu is correct for the low turbulence gas flow. In the case of the high turbulence gas flow (for example, it may be done by the special unit with the same profile as the target rod, placed between the target and the inlet of cooling gas), calculated Nu should be 1.5–2 times increased [10] and thus decreasing of Nu due to longitudinal cooling may be compensated.

Calculations show that at the gas velocity 10 m/s the heat transfer coefficient is about 100 W/m^2/K for air (nitrogen) and 300 W/m^2/K for helium.

2.3.2 Target Design

The target design with longitudinal gas cooling is shown in Figure 2.10. The target core consists of nine 10 cm length rods (or six 15 cm length rods) with a rib height approximately equal to 8.6 mm so that an internal diameter of the target casing is equal to 23.6 mm (specified stainless steel pipe 24 mm in diameter and 0.2 mm wall thickness). It corresponds to average temperatures of ∼300°C and ∼270°C for graphite and beryllium targets respectively even for $\alpha_g = 100$ W/m^2/K [2]. Two beryllium windows seal and separate the target core from an environment atmosphere. The cooling gas passes through the inlet pipe with necessary velocity. In order to have a higher degree of the gas turbulence, each following rod is rotated to an angle equal to 22.5° with respect to preceding one. Gas outlet is coaxial with the inlet cooling channel. The thickness of the external pipe is equal to 0.3 mm; the external diameter is equal to 30 mm.

The target rod may be made from graphite, as well as from beryllium, but from the point of view of the cost, graphite may be preferable because its machining does not requires a special license. In order to prevent an erosion, the graphite rod should be coated with a thin film. Alumina plasma-sprayed in vacuum is the most suitable material for coating. It has

[2] For comparison, average temperatures of the HE target are equal to ∼350°C and ∼170°C for graphite and beryllium respectively [3].

high radiation resistance, high strength and, that is important, practically the same as graphite coefficient of a thermal expansion ($6.7 \cdot 10^{-6}$ [9]).

It is necessary to note, that there is no reason to achieve the limited value 40 mm of an external diameter, because in the range of acceptable gas velocities of 10–20 m/s it is impossible to reach the total flow rate of 20–40 l/s, providing not very high temperature of the target (see Table 2.1). An increasing of the mass of a cooling gas may be achieved by an increasing of the pressure in the cooling system. The following assumptions have been made [13]:

- gas pressure P, density ρ and absolute temperature T satisfy to the Klapeyrone law: $P = RT\rho$, where R is the gas constant;
- coefficient of a dynamic viscosity μ is the function of absolute temperature T only: $\mu/\mu_0 = (T/T_0)^{0.75}$;
- specific heats C_p and C_v do not depend on temperature and are the physical constants of a cooling gas;
- heat conductivity λ_g is proportional to coefficient of a dynamic viscosity μ so that Prandtle number $Pr = \mu C_p/\lambda_g$ is the constant equal to 0.722 (air or nitrogen) and 0.667 (helium).

As it follows from the results of calculations of a temperature rise of a cooling gas as a function of a static pressure in the cooling system (Figure 2.11), at a static pressure about 1.0–1.2 MPa the temperature rise of a cooling gas (nitrogen) is about 60°C under flow rate of 4 l/s (gas velocity is equal to 20 m/s). The maximum target temperature in this case will be about 320°C. This value is comparable with the temperature of the HE target with water cooling [3]. Estimations of stresses in a target with gas cooling according given above formulas show that for higher average temperatures the equivalent stresses are slightly lower (about at 5–10%).

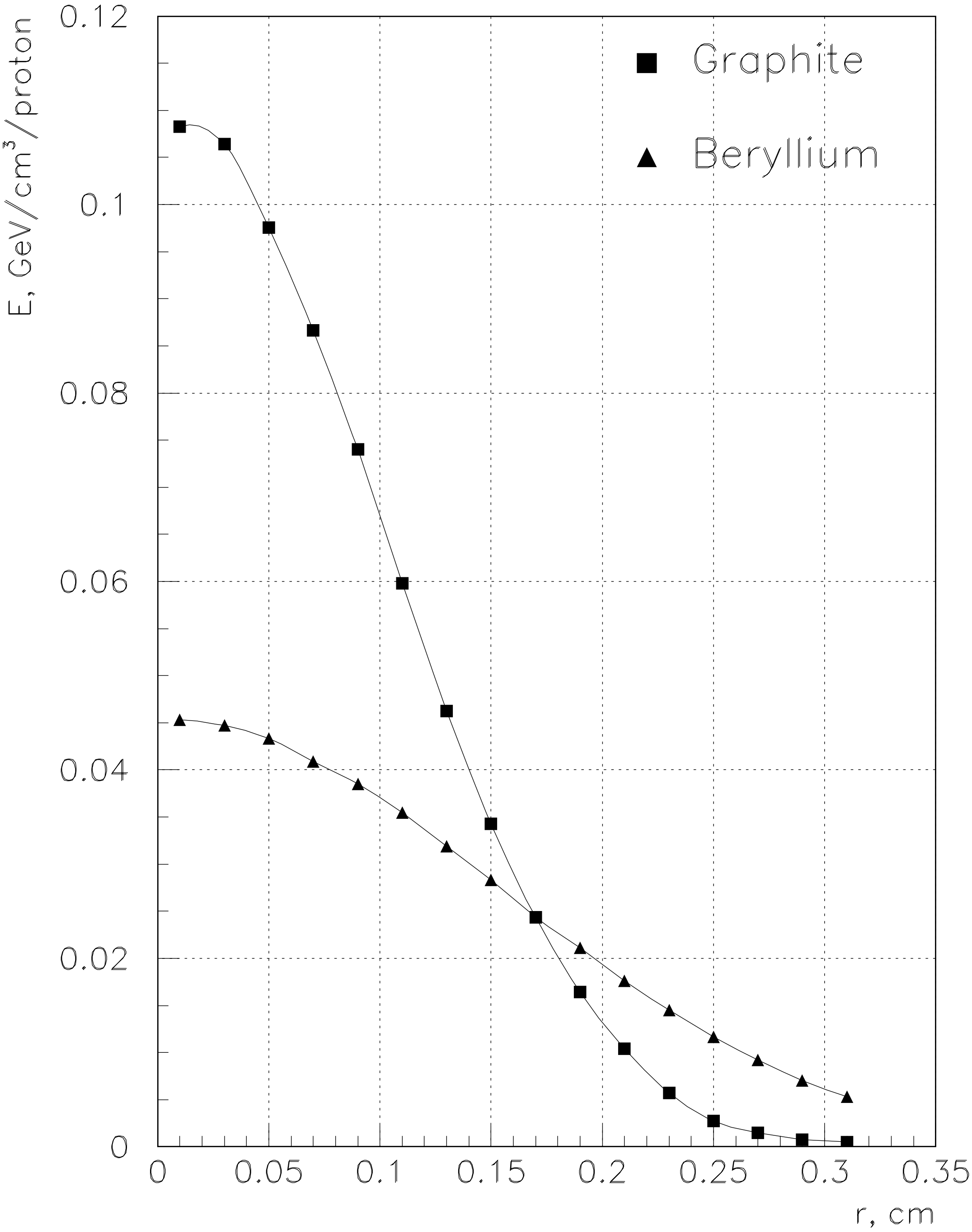

Figure 2.1: Radial distributions of the energy deposition density in the rod targets.

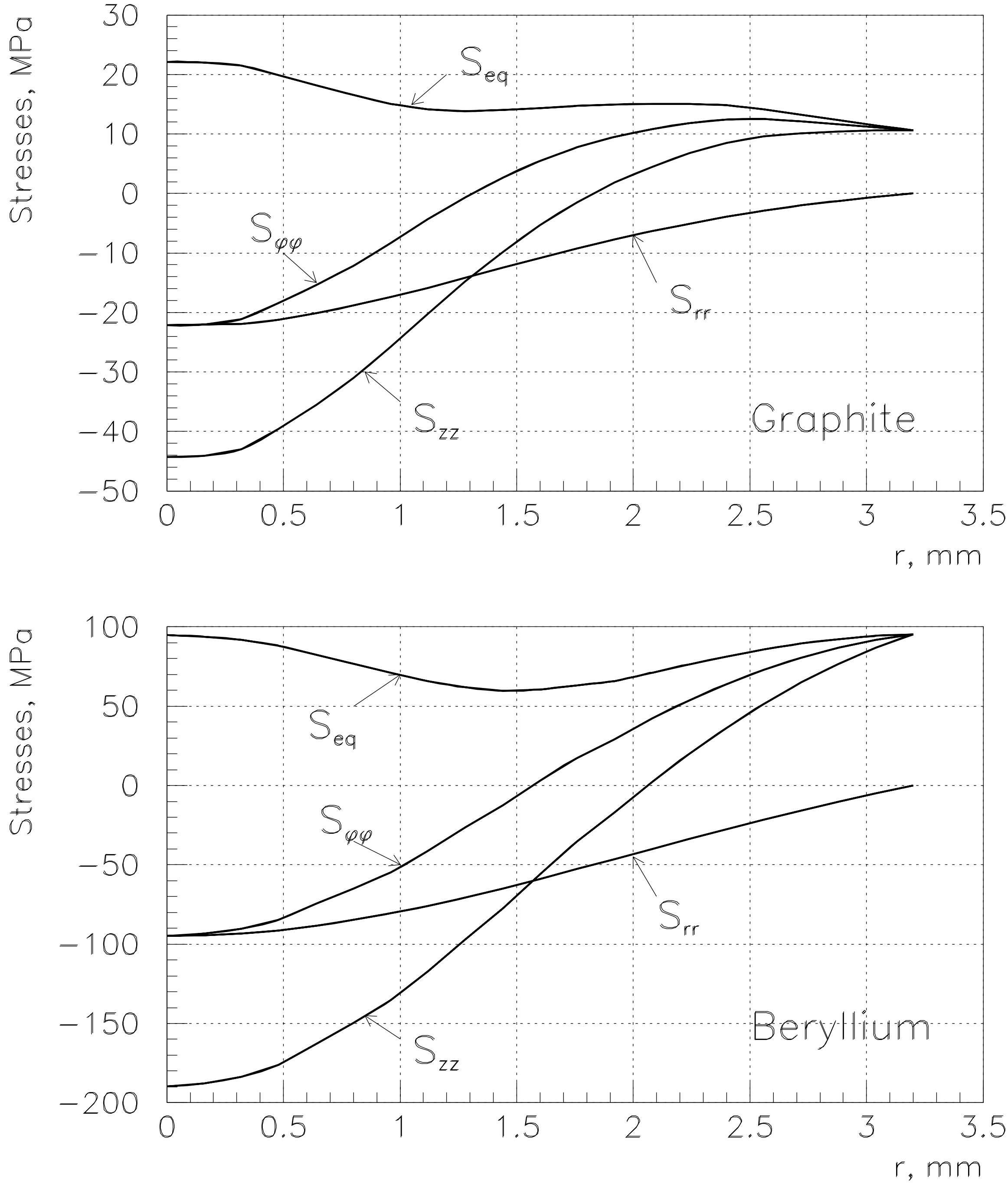

Figure 2.2: Stresses in the cylindrical target.

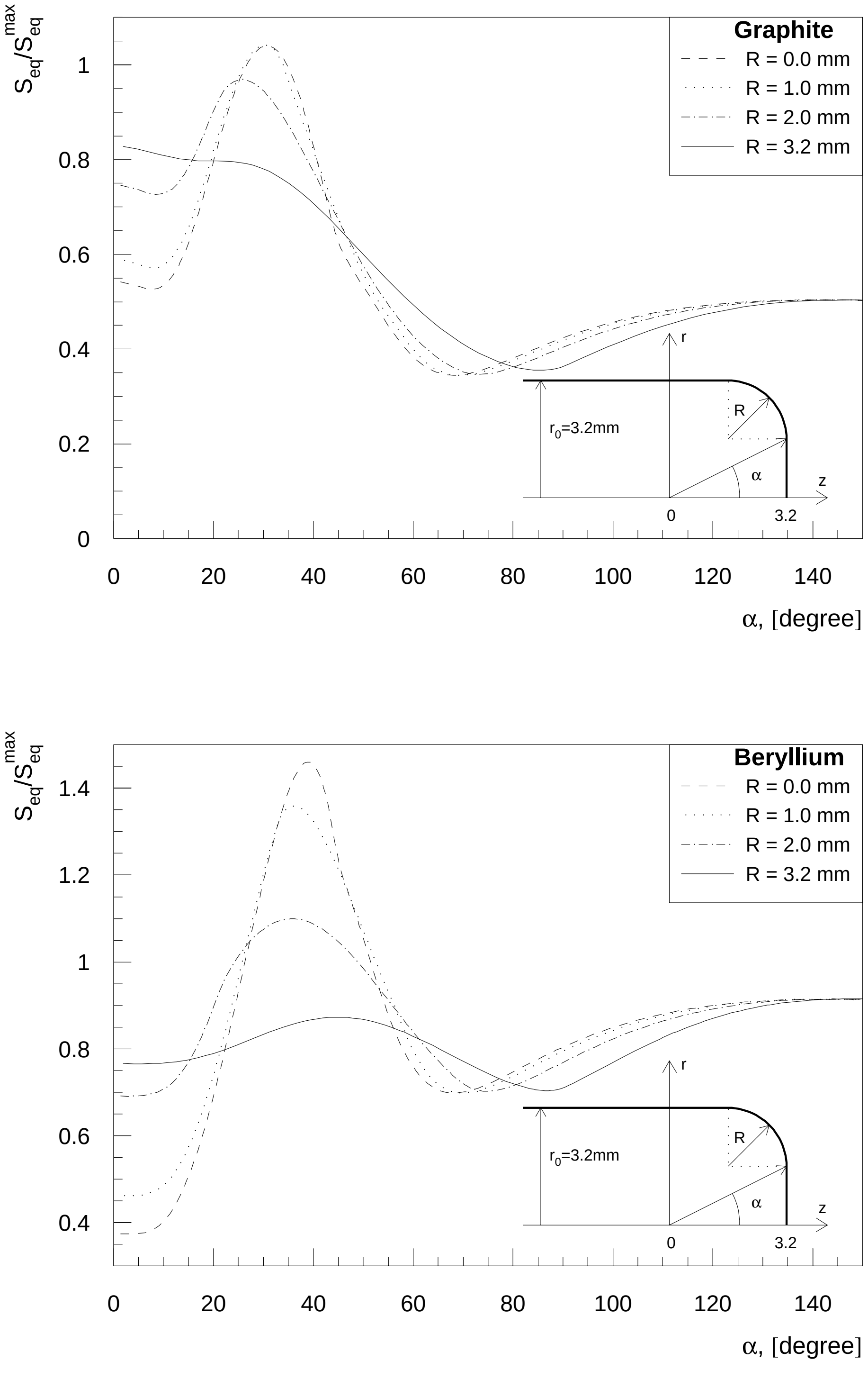

Figure 2.3: Stress concentration at the target ends.

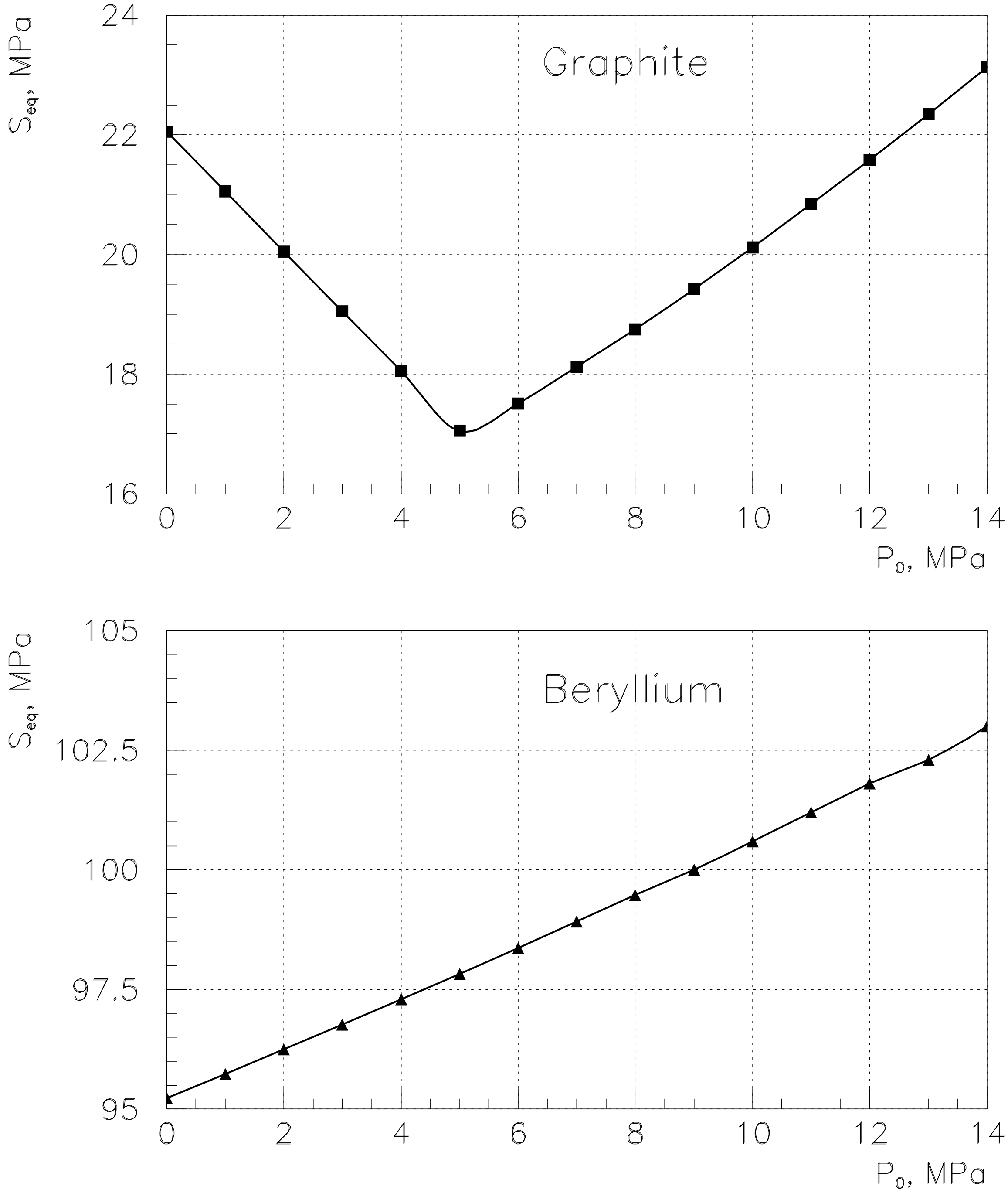

Figure 2.4: Maximum equivalent stress as a function of the prestress value.

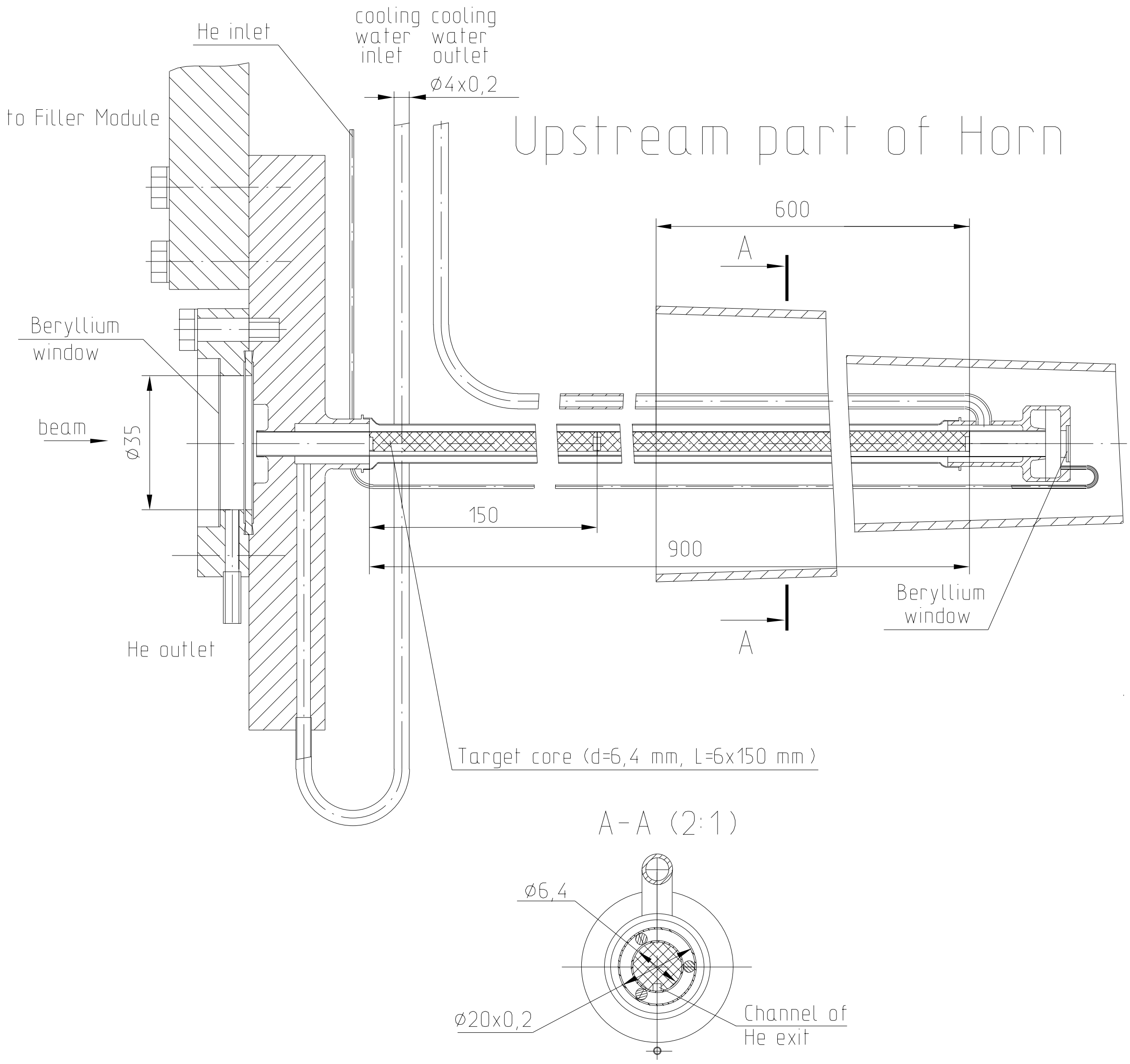

Figure 2.5: Water cooled target with a cylindrical core and separate outlet water channel.

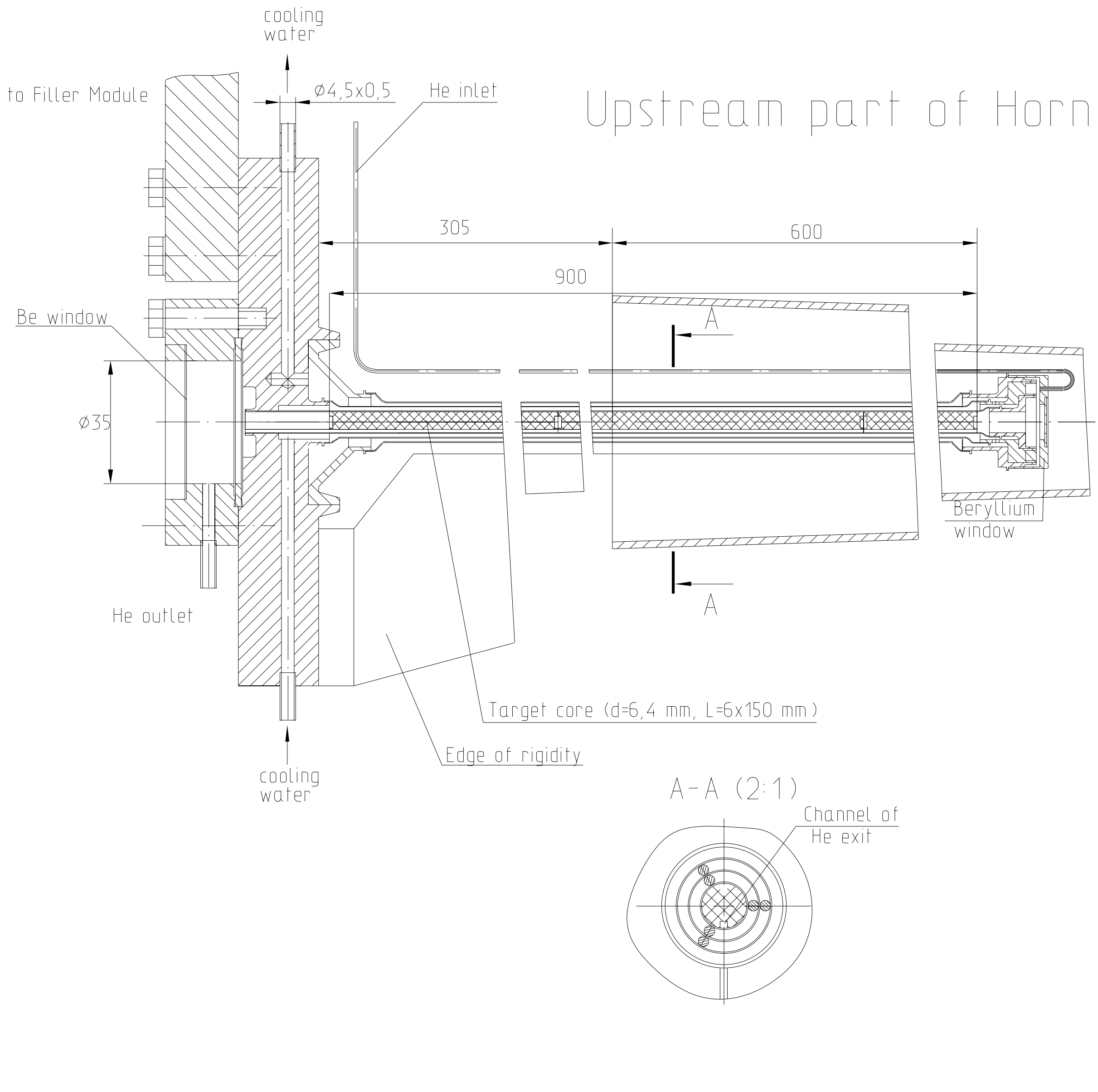

Figure 2.6: Water cooled target with a cylindrical core and coaxial outlet water channel.

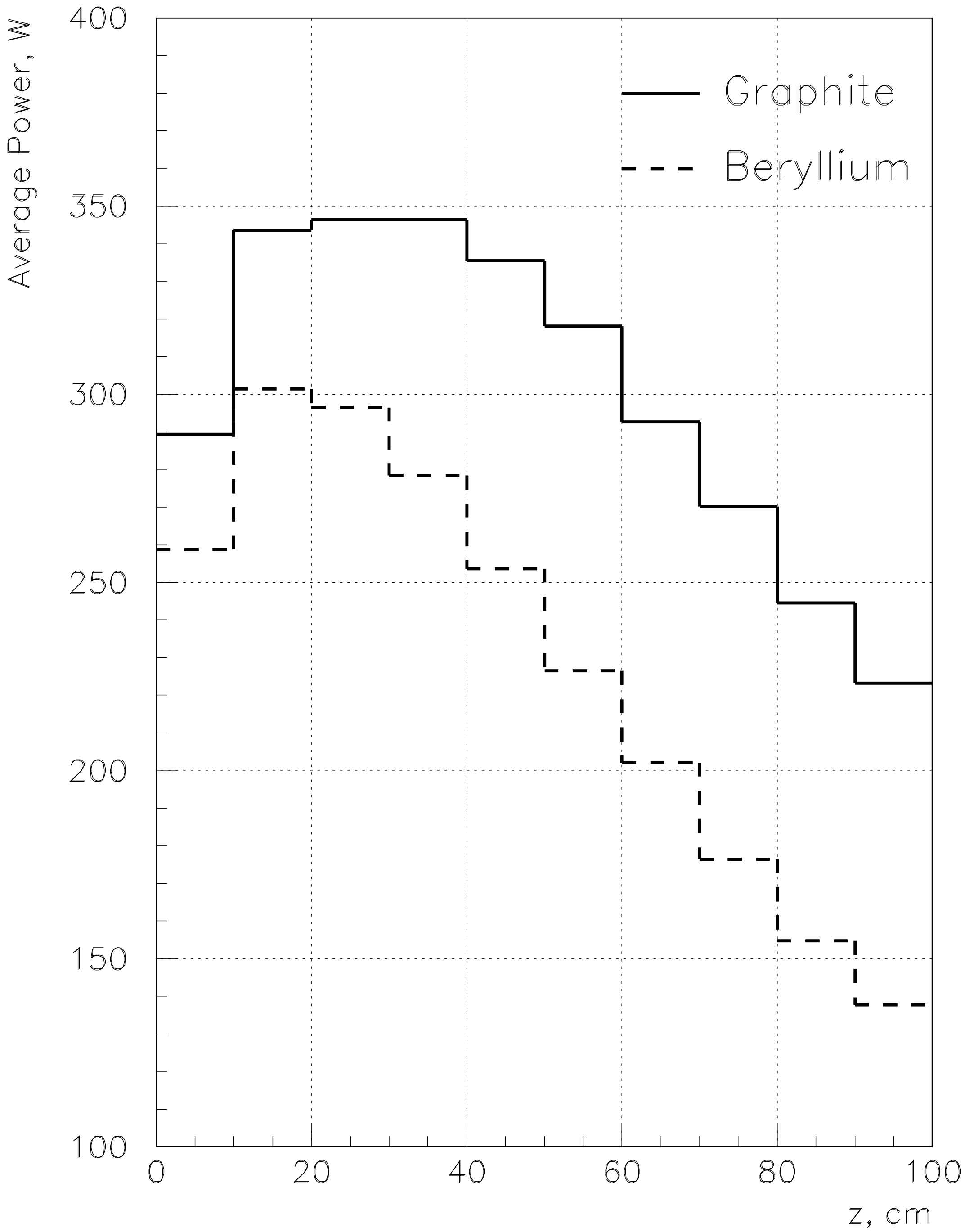

Figure 2.7: Longitudinal distribution of the average deposited power.

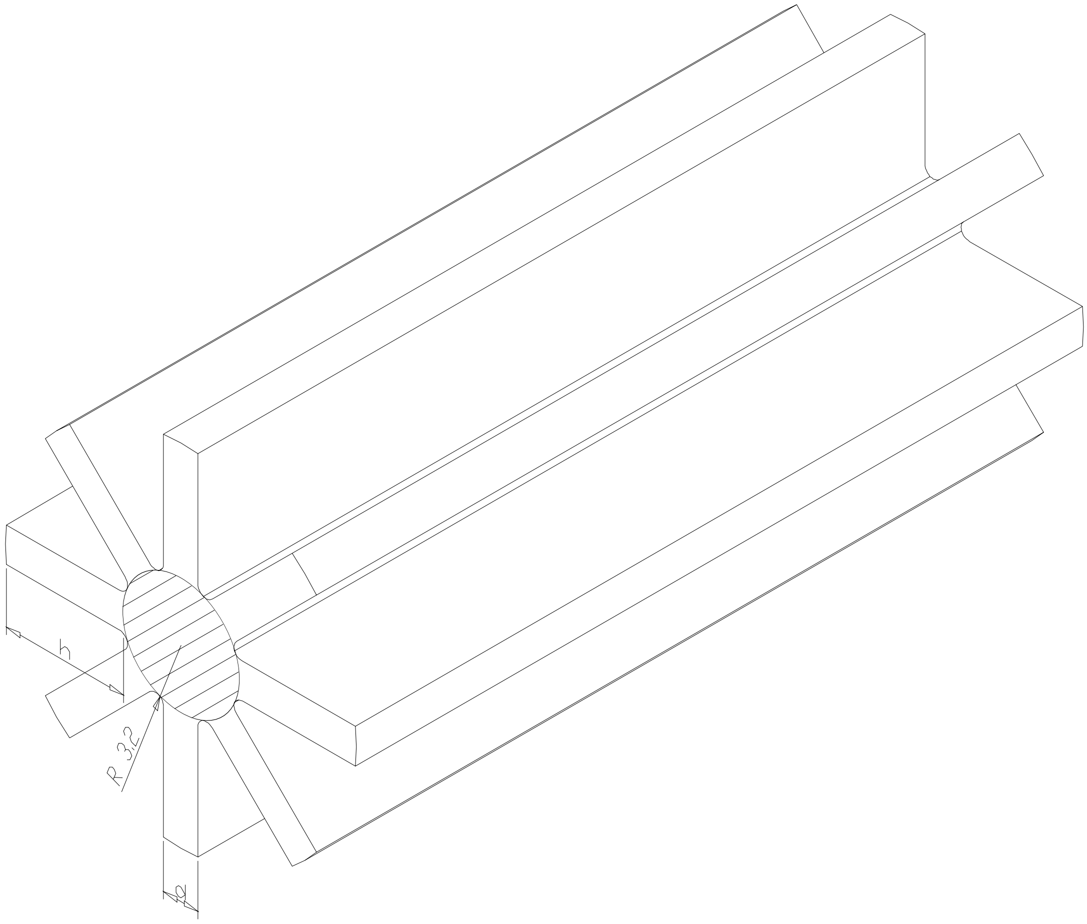

Figure 2.8: Radiator for the cylindrical target with gas cooling.

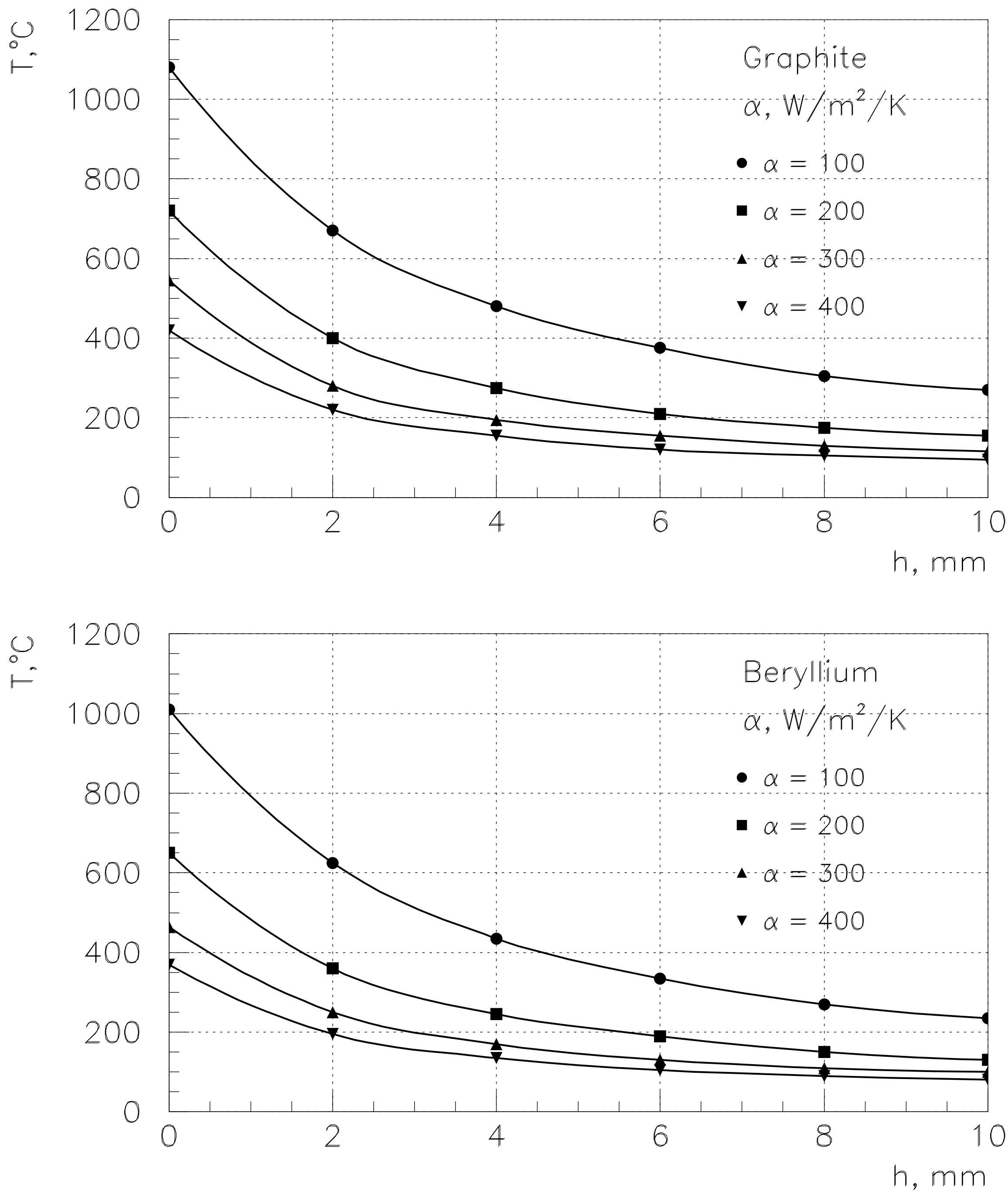

Figure 2.9: Average target temperature as a function of the rib height of the radiator.

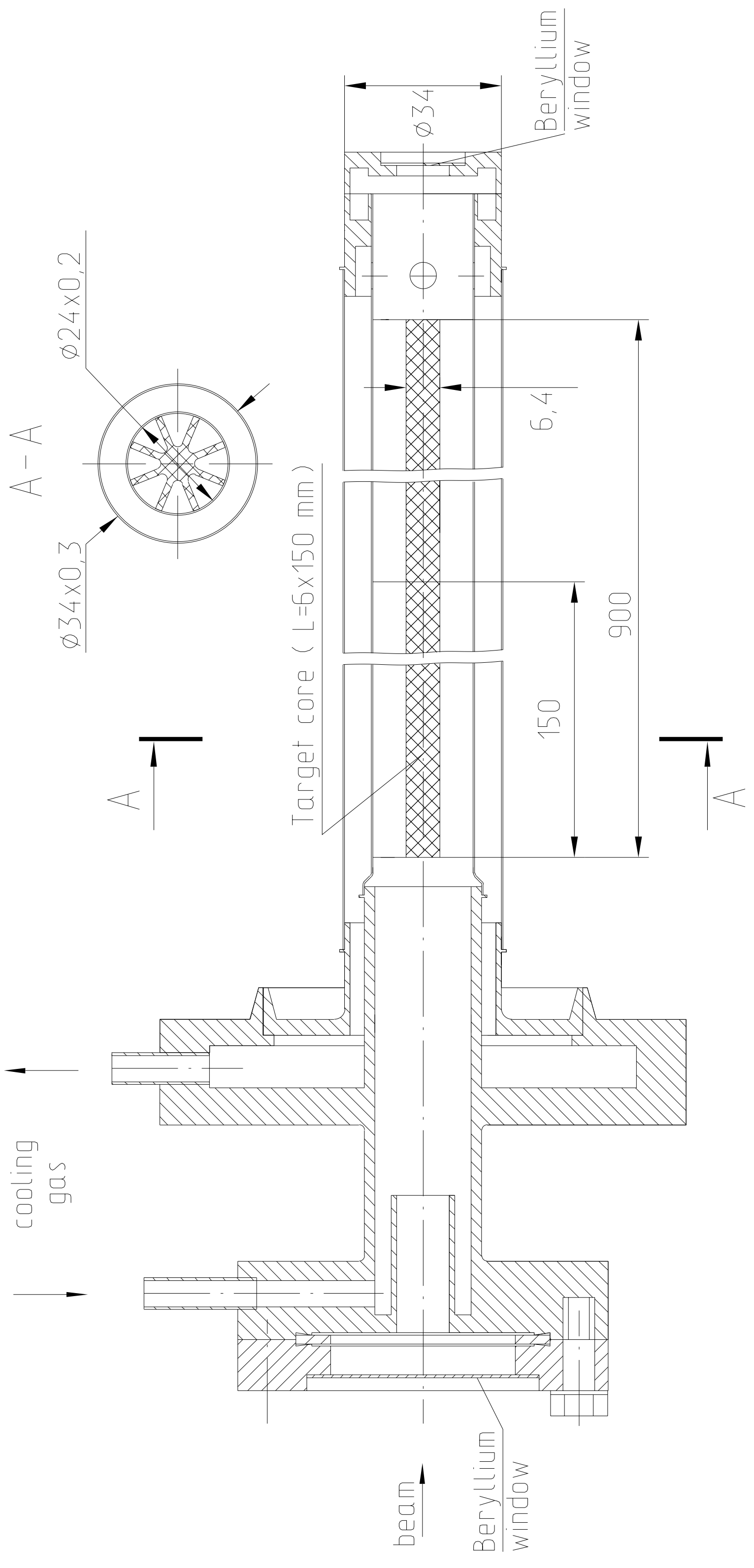

Figure 2.10: Gas cooled target with a cylindrical core.

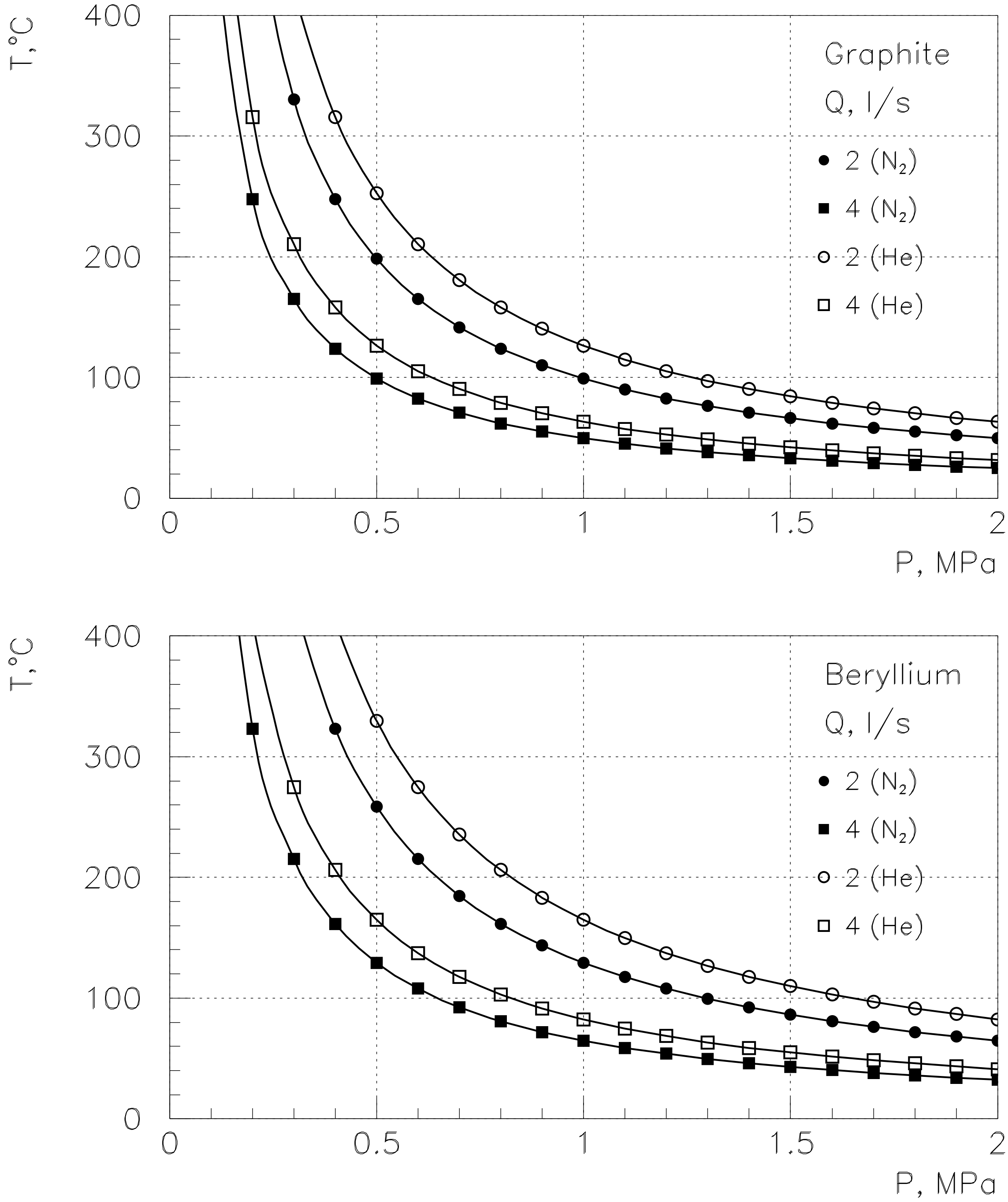

Figure 2.11: Temperature rise of a cooling gas as a function of static pressure in cooling system.

3 LE Targets with Fin Core

Properties of the LE fin target are similar to ones for ME and HE targets:

- the target should be cut into teeth along the beam in order to decrease the stresses in the target;
- the target should be placed in a vacuum-tight envelope filled with neutral atmosphere to prevent an oxidation and weight losses of graphite or beryllium.

As it was shown above (see Figure 1.3 of Section 1) optimal thicknesses of LE fin targets are equal to 3.2 mm and 4.1 mm for graphite and beryllium respectively.

Distributions of the energy deposition in a cross section of the target, as well as those of stresses in a target tooth strongly depend on the transversal proton beam distribution in the target. Two types of beam distributions have been considered:

- vertical beam dispersion in the target $D_y = 0$;
- horizontal beam dispersion in the target $D_x = 0$.

3.1 Target with Water Cooling

The stress calculations were made for the model given in Figure 3.1 at the heat transfer coefficient to water equal to 10 kW/m^2/K and wall thickness of cooling pipes equal to 0.2 mm.

3.1.1 Graphite Target

1) $D_y = 0$. In this case the distribution of the energy deposition density in the X-direction is quite symmetrical (Figure 3.2). The optimum length of a tooth is equal to 6.54 mm as it follows from the dependencies of stresses in a target tooth as a functions of its length. The equivalent stress for this length of the tooth is equal to 17.1 MPa.

Because σ_y of a proton beam for the base line graphite target is equal to 1.4 mm, decreasing of the energy deposition density can be achieved by increasing of σ_y up to its maximum possible value of 2.0 mm. Calculations of stresses in the tooth of the ME target for $\sigma_y = 2.0$ mm and $\sigma_x = 0.7$ mm show that in this case maximum equivalent stress takes place in the tooth center and its value is ~1.3 times less than for $\sigma_y = 1.4$ mm. Similar results may be expected for the LE target too.

2) $D_x = 0$. In this case the distribution of the energy deposition density in the horizontal plane is asymmetrical (Figure 3.3), but for given σ_x its amplitude is ~1.2 times less than for $D_y = 0$. The minimum equivalent stress of 17 MPa takes place at the length of a tooth equal to ~10 mm.

Of course, for both cases ($D_x = 0$ and $D_y = 0$) the optimum lengths of a tooth are relatively small to realize it in the target construction. It is more reasonable to increase the tooth length despite of stress increasing. If we shall take $L_t = 20$ mm, stresses will be equal to 22.5 MPa ($D_x = 0$) and 27.5 MPa ($D_y = 0$). Such increase of stresses is not very serious, because the fatigue stress limit for the ZXF–5Q graphite can be estimated at the order of 36 MPa [14], i.e. for the beam distribution with $D_x = 0$ it corresponds to the safety factor of 1.6.

3.1.2 Beryllium Target

1) $D_y = 0$. Similar to the graphite target the distribution of the energy deposition density is quite symmetrical (Figure 3.4); optimum length of the target tooth is equal to 8 mm at the equivalent stress of 130 MPa.

2) $D_x = 0$. The amplitude of the energy deposition density is ~1.2 times less than for $D_y = 0$ (Figure 3.5). The optimum length of a tooth is equal to 11.5 mm, and corresponding equivalent stress is equal to 112 MPa. For the equivalent stress of 130 MPa, the length of a tooth will be equal here to 16.5 mm.

Parameters of considered beams and targets are summarized in the Table 3.1. For comparison, the sensitivity of the proton beam location in the target to the linear and angular positions of the beam at the output of the Main Injector are given too.

Analysis of this table shows that for both target materials focusing of the proton beam in the target with $D_x = 0$ is preferable not only due to target characteristics but also from the point of view of the beam stability in the target. In the case of $D_x = 0$ the stability of the beam in the horizontal direction is ~2.3 times higher than for $D_y = 0$.

Beam parameters	Graphite		Beryllium	
σ_x (mm)	0.70	0.70	1.0	1.03
σ_y (mm)	1.40	1.40	2.00	2.02
D_x (mm/%Δp/p)	16.25	0.00	16.00	0.00
D_y (mm/%Δp/p)	0.00	22.14	0.00	5.87
$\Delta X/\Delta X_s$	1.02	–0.47	0.68	–0.68
$\Delta X/\Delta X'_s$ (mm/0.1mrad)	–1.86	–0.72	–2.33	–1.04
$\Delta Y/\Delta Y_s$	–2.88	–2.85	–4.08	–4.05
$\Delta Y/\Delta Y'_s$ (mm/0.1mrad)	–3.74	–4.08	–5.46	–5.32
Magnet	Strength (kG/m)			
Q6	57.56	51.67	68.36	57.99
Q7	–63.44	–61.14	–75.29	–68.13
Q8	–84.32	–83.63	–81.40	–76.25
Q9	97.70	89.24	91.38	81.99
Q10	–18.17	–11.94	–9.66	–8.61
Target				
S_{eq} (MPa)	27.50	22.50	130.00	130.00
L_t (mm)	20.00	20.00	8.00	16.50

Table 3.1: Parameters of the proton beam for fin targets.

3.1.3 Target Design

Contrary to the medium and high energy targets there is no space in the low energy target design to locate the cooling system similar to that used for HE and ME targets [3]. Only one way exists to provide a good thermal contact between the target core and a cooling pipe: brazing of water cooling pipes to the target material (beryllium or graphite).

This design is shown schematically in Figure 3.6. The total length of the target material is equal to 900 mm and consists of 45 teeth (each 20 mm length) for the graphite target and 55 teeth (each 16.4 mm length) for beryllium one. Each tooth has radius of rounding made by an electrical discharge machine and equal to the half of fin thickness. Target teeth are brazed to cooling pipes by hard solder heated by an electron beam in a vacuum. The target is located in the 26–30 mm in diameter vacuum-tight stainless steel pipe filled with helium, which should be supplied from the downstream end of the pipe. Two beryllium windows seal and separate an internal target volume from a surrounding environment. Version 3 from a possible variety of cooling is preferable for beryllium target because diameter of a cooling pipe is comparable with the thickness of a target fin. Version 4 may be used for the graphite target.

The power, deposited along the fin target in terms of average power is shown in Figure 3.7. The total power is equal to 2.7 kW for the graphite target and 2.6 kW for beryllium one.

Parameters of the cooling system for the fin target design depend on hydraulic diameter of a cooling pipe d_h and average velocity v of cooling water. A heat transfer coefficient may be defined via Nusselet, Prandtle and Reynolds numbers from formulas given above. A pressure drop in terms of water column at the length of a pipe $L \simeq 2$ m may be calculated as

$$H = \Lambda \frac{L}{d_h} \frac{v^2}{2g},$$

where Λ is the hydraulic coefficient of friction. Λ for turbulence flow may be calculated in a wide range of Reynolds numbers for given roughness Δ of a pipe as [10]

$$\Lambda = 0.11 \left(\frac{\Delta}{d_h} + \frac{68}{Re} \right)^{0.25}.$$

The possibility of target cooling was investigated for version 3 (Figure 3.6). Dependencies of a heat transfer coefficient, a pressure drop for roughness of a pipe $\Delta = 0.02$ mm, a total water flow rate and a temperature rise for the graphite target as functions of the hydraulic diameter for different water flow velocities are shown in Figures 3.8–3.11 respectively.

As it follows from Figure 3.8 the value of a heat transfer coefficient ≥ 10 kW/m^2/K can be provided in a wide range of diameters of pipes and water flow velocities. It is reasonable to take $d_h = 4$ mm. In this case at a water velocity equal to 3.5 m/s, the water temperature rise is equal to 17°C (Figure 3.11), the total water flow rate is equal to 2.3 l/min (Figure 3.10) at a pressure drop equal to 0.87 atm (Figure 3.9). On the other hand, increasing of a channel diameter to 5 mm gives temperature rise of 11°C, a total water flow rate of 3.5 l/min at a pressure drop equal to 0.68 atm that may be more reasonable for the target design. More careful analysis of water cooling system should be done at the stage of the advanced conceptual design in order to take into account the influence of an average temperature to a sag of the target design.

3.2 Target with Gas Cooling

The problems arisen under cooling of the target with a fin core are practically the same as for the LE target with a cylindrical core.

3.2.1 Target Cooling

As in the case of a cylindrical target core, in order to obtain effective gas cooling it is necessary to increase the area of heat exchanging between the cooling gas and target core. During designing one should take into account that a target fin is cut into teeth to decrease the stresses in a target. Schematical view of a possible design of the target core is given in Figure 3.12. It consists of two identical parts clamped together and thus allows to obtain the target density as much as possible. Increasing of the heat exchanger area is achieved by four ribs of a height h. The dependencies of an average target temperature on a rib height h for two thicknesses of rib and heat transfer coefficients equal to 100 W/m^2/K (nitrogen) and 300 W/m^2/K (helium) are shown in Figure 3.13. Analysis of this data shows the following:

- the target temperature is slightly depends on the thickness of a rib. It means that 2 mm thick rib is preferable because the ribs with higher thickness will give additional losses of a target luminosity;
- at a height of a rib equal to 12 mm it is possible to apply nitrogen as a cooling gas; temperature of the target is equal to $\sim$250°C. For comparison, the temperature of the HE fin target with combined cooling (heat conductivity plus forced water cooling) is equal to $\sim$170°C.
- under helium cooling a height of a rib may be essentially less than for the nitrogen one. A height of a rib equal to 5 mm is quite enough for the same average temperature of the LE target as in the HE one.

Similar to the LE target with the cylindrical core, a temperature rise of a cooling gas at flow velocities of the order of 10–20 m/s, is also too large. To reduce the temperature rise of a cooling gas and consequently the target temperature, it is necessary to use a cooling system operating at a high static pressure of a cooling gas.

3.2.2 Target Design

The design of the gas cooling LE fin target is given in Figure 3.14. A height of a 2 mm thick rib was chosen equal to 12 mm. In order to provide a good thermal contact between target teeth and a rib, they should be brazed together or machined out from a solid piece that looks preferable for the graphite target. The target consists of six 150 mm length segments. Each segment is an assembly of two identical units (rib with teeth) clamped together via three 12 mm height rods. Target segments are inserted into the 30 mm in diameter and 0.2 mm thick stainless steel pipe. A diameter of the external pipe is equal to 38 mm; the wall thickness is equal to 0.3 mm.

A length of a tooth was defined from calculations of stresses for the proton beam with zero horizontal dispersion in the target ($D_x = 0$). In these calculations a heat transfer coefficient between the cooling gas and target was equal to 100 W/m^2/K, while the temperature rise of a cooling gas did not take into account. The equivalent stresses in a most critical points of target tooth as a function of its length are shown in Figure 3.15 (positions of points 1, 2, 3 are given in Figure 3.1.). Analysis of stresses shows:

- an optimum length of a tooth for the graphite target is equal to $\sim$12 mm and is defined by the stress value at the point 2 ($\pm$d/2,0,0). In the case when a tooth length is equal to 20 mm (as for the target with water cooled fin core), an equivalent stress increases to 20.7 MPa. Finally, the length of a target tooth should be chosen at the stage of the advanced conceptual design;

- a length of a tooth in the beryllium target is defined by the stress on its lateral surface (point 2) similar to the graphite target. In the range of tooth lengths from 12 to 16 mm the equivalent stress varies only from 127 MPa to 135 MPa. Therefore the length of the tooth may be chosen in a range of 12–16 mm.

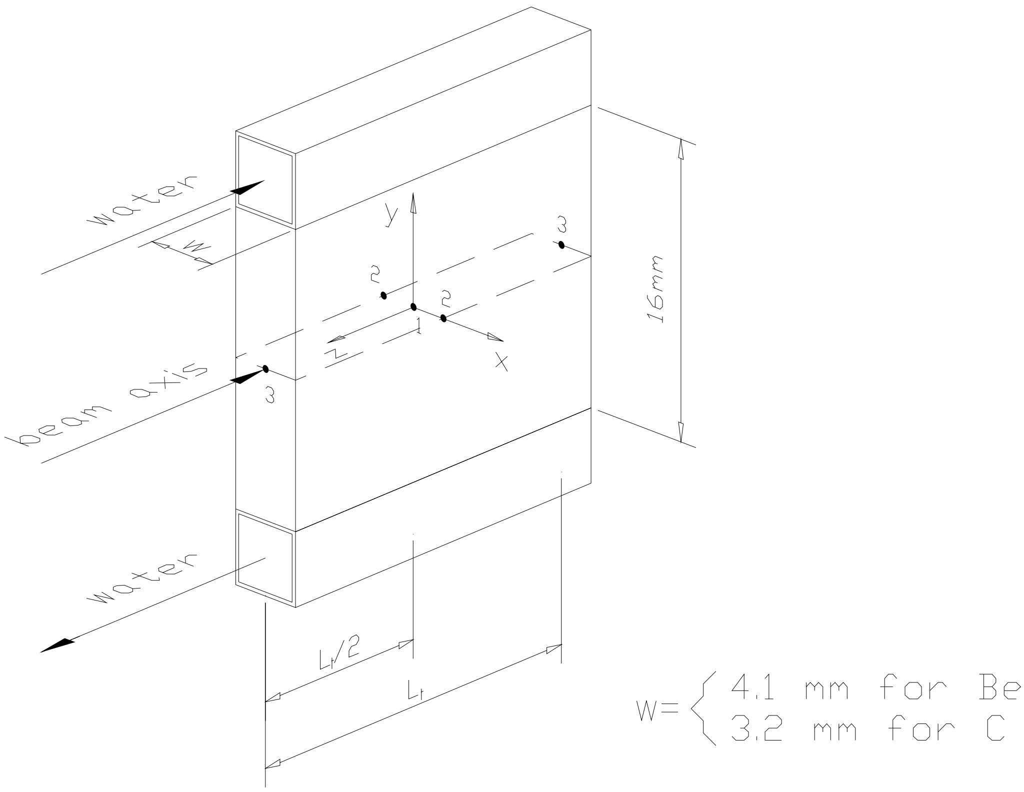

Figure 3.1: Model of a target tooth for temperature and stress calculations.

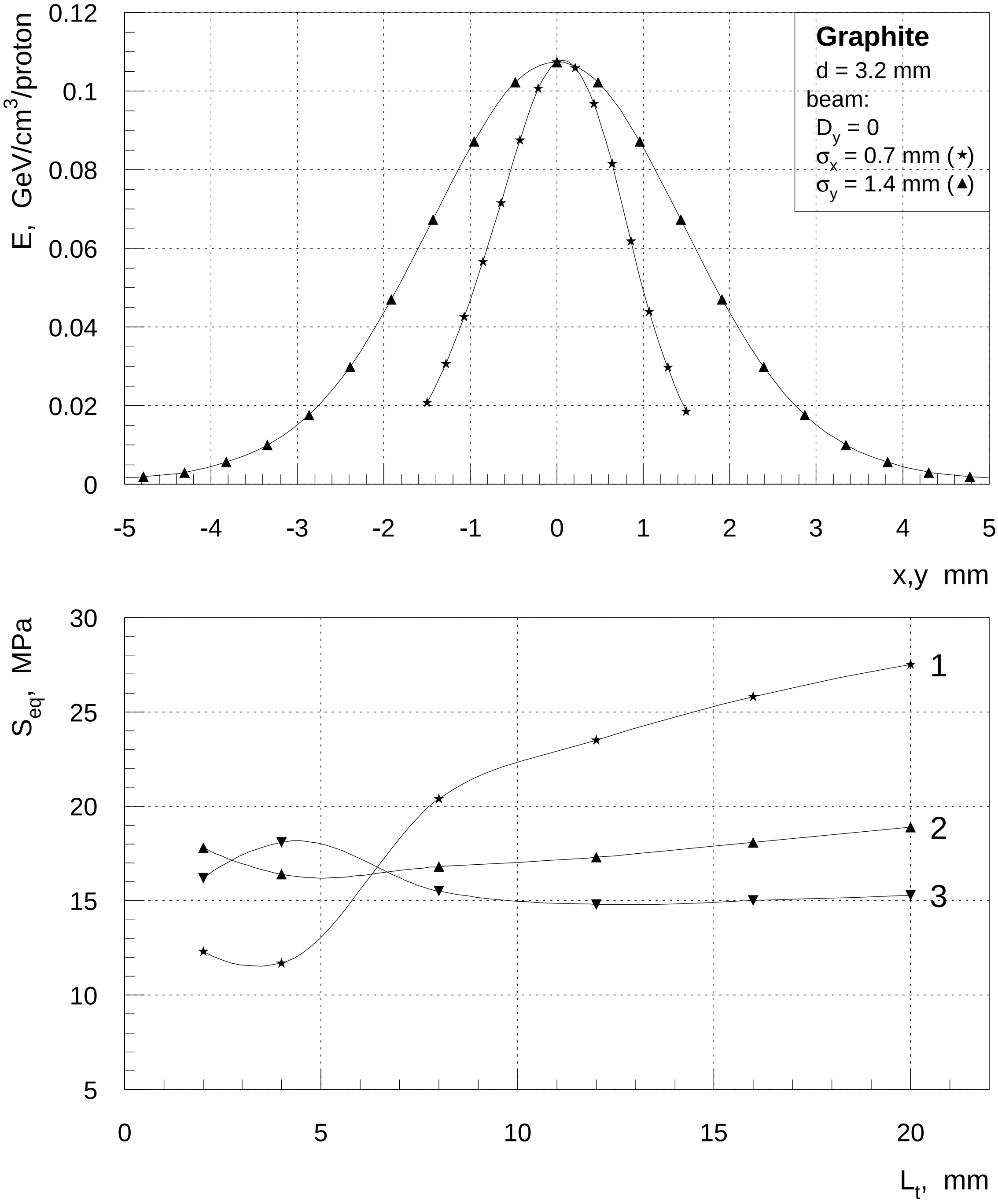

Figure 3.2: Distributions of density of energy deposition in transverse directions of the graphite target and equivalent stresses versus of the teeth length. Proton beam dispersion $D_y = 0$. Points 1, 2, 3 — see Figure 3.1.

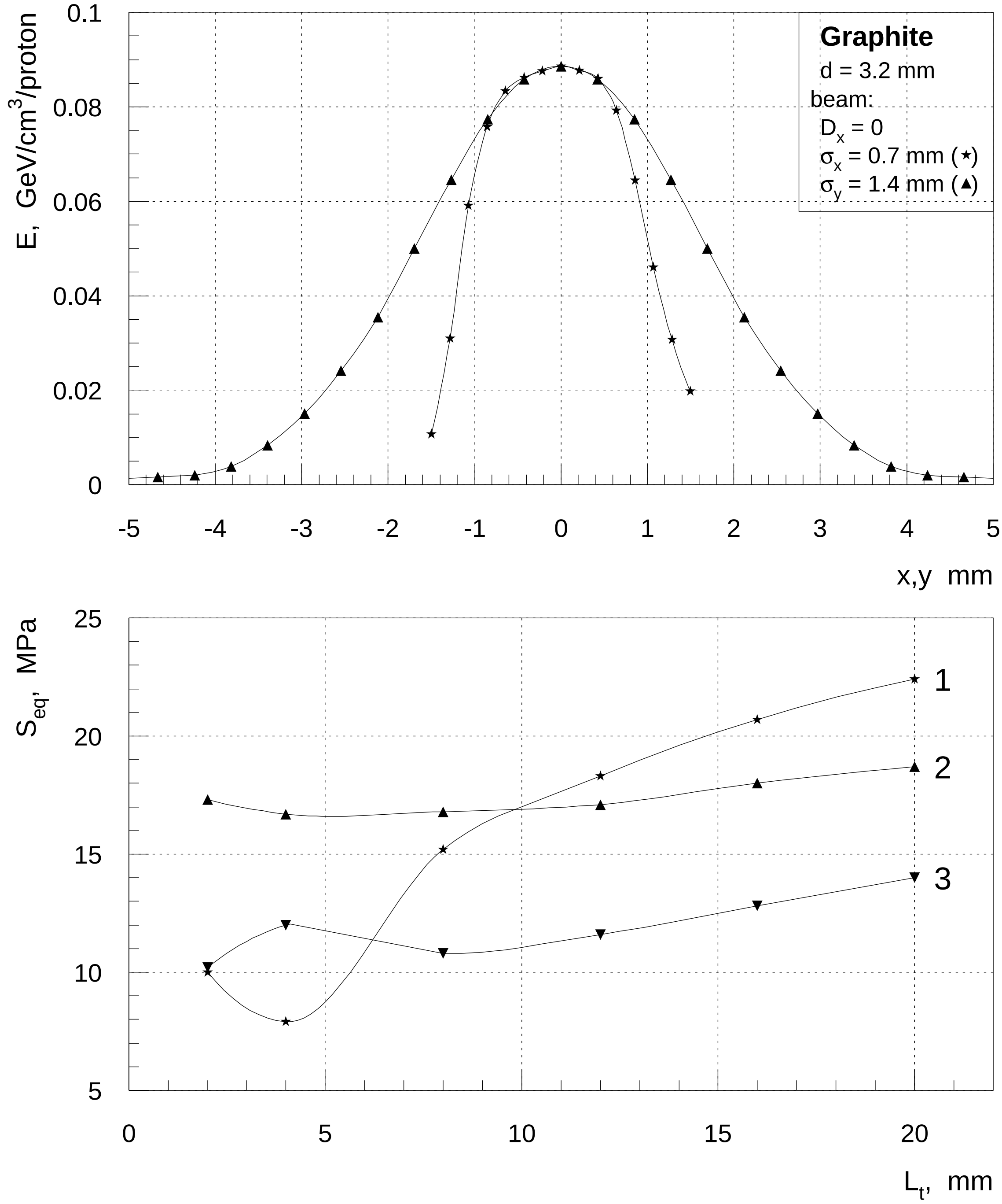

Figure 3.3: Distributions of density of energy deposition in transverse directions of the graphite target and equivalent stresses versus of the teeth length. Proton beam dispersion $D_x = 0$. Points 1, 2, 3 — see Figure 3.1.

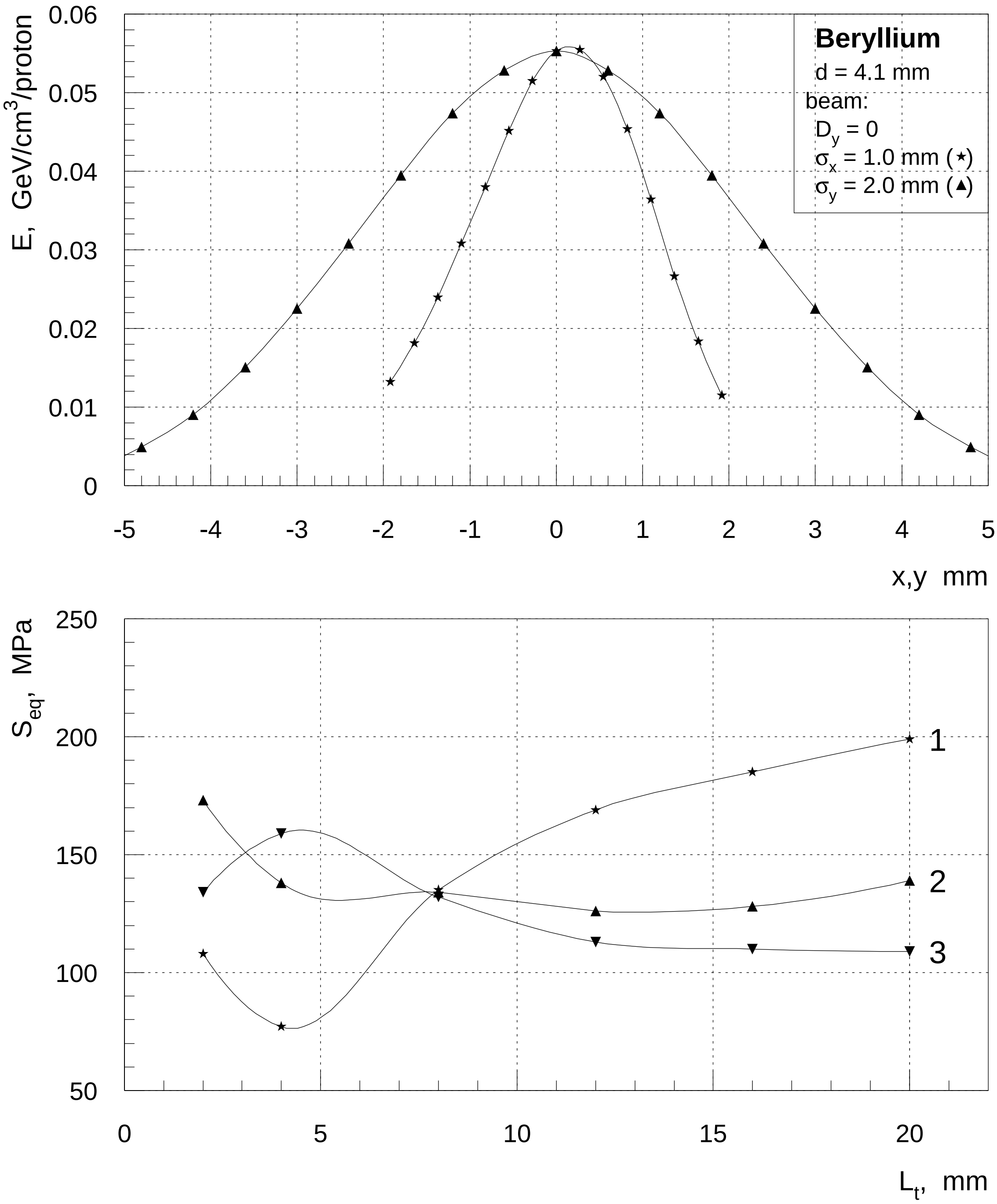

Figure 3.4: Distributions of density of energy deposition in transverse directions of the beryllium target and equivalent stresses versus of the teeth length. Proton beam dispersion $D_y = 0$. Points 1, 2, 3 — see Figure 3.1.

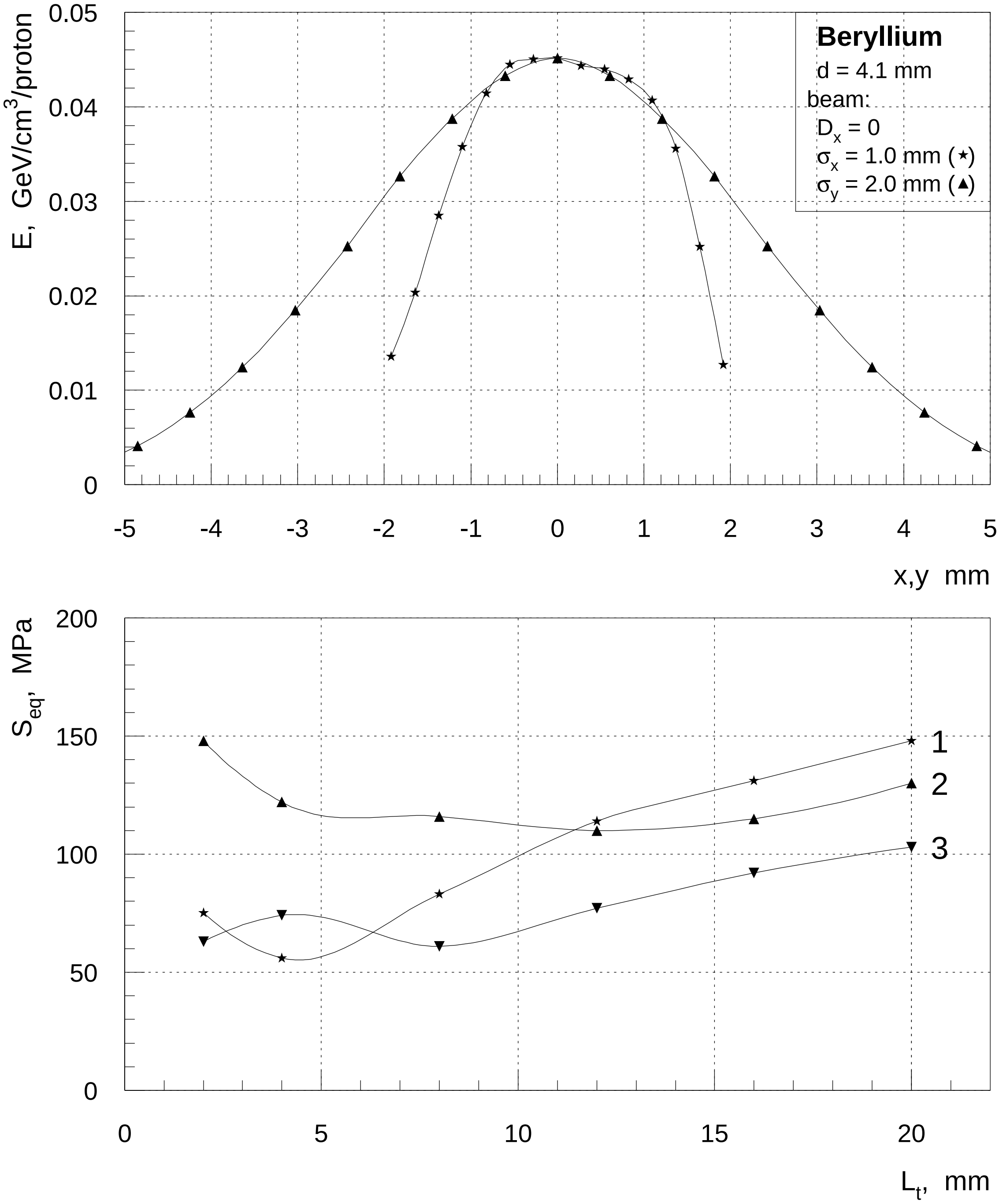

Figure 3.5: Distributions of density of energy deposition in transverse directions of the beryllium target and equivalent stresses versus of the teeth length. Proton beam dispersion $D_x = 0$. Points 1, 2, 3 — see Figure 3.1.

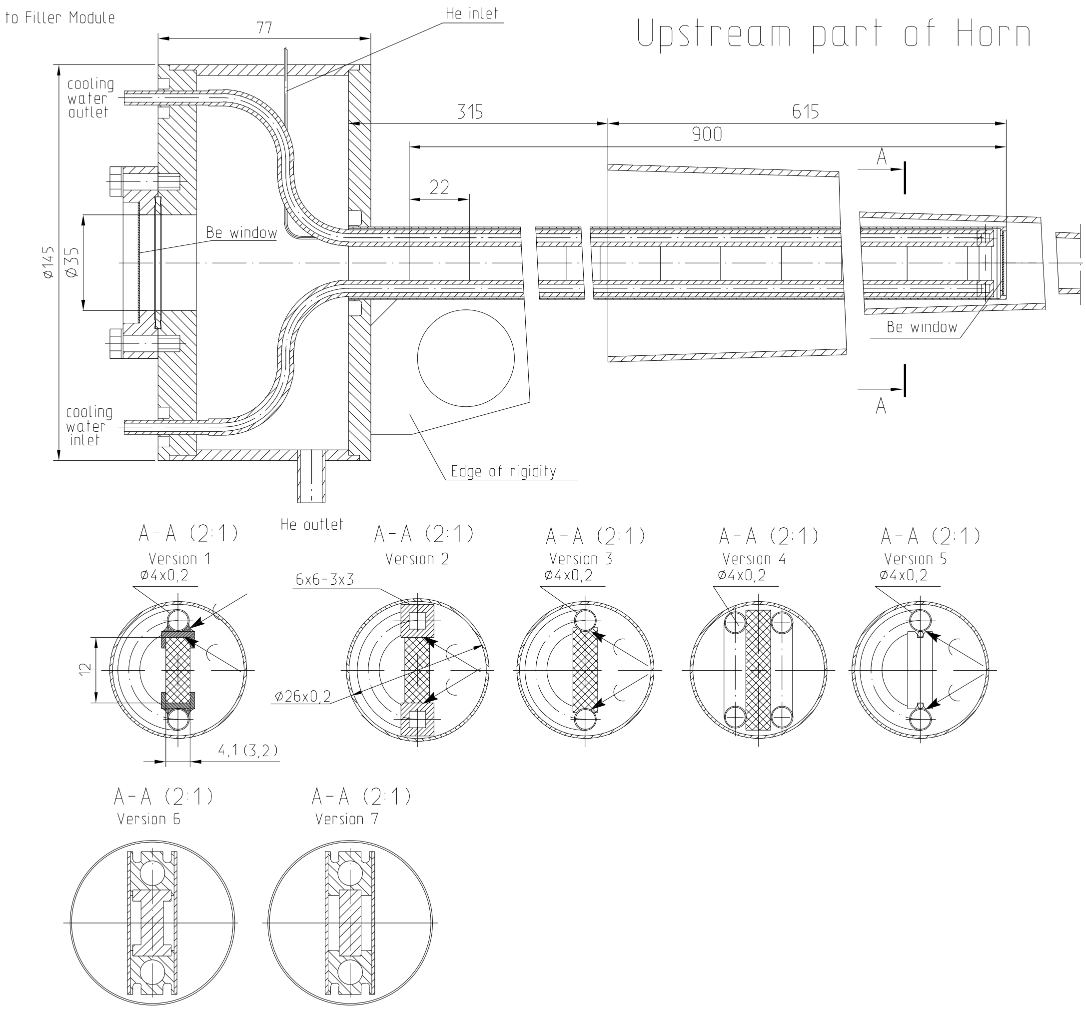

Figure 3.6: Fin target with water cooling.

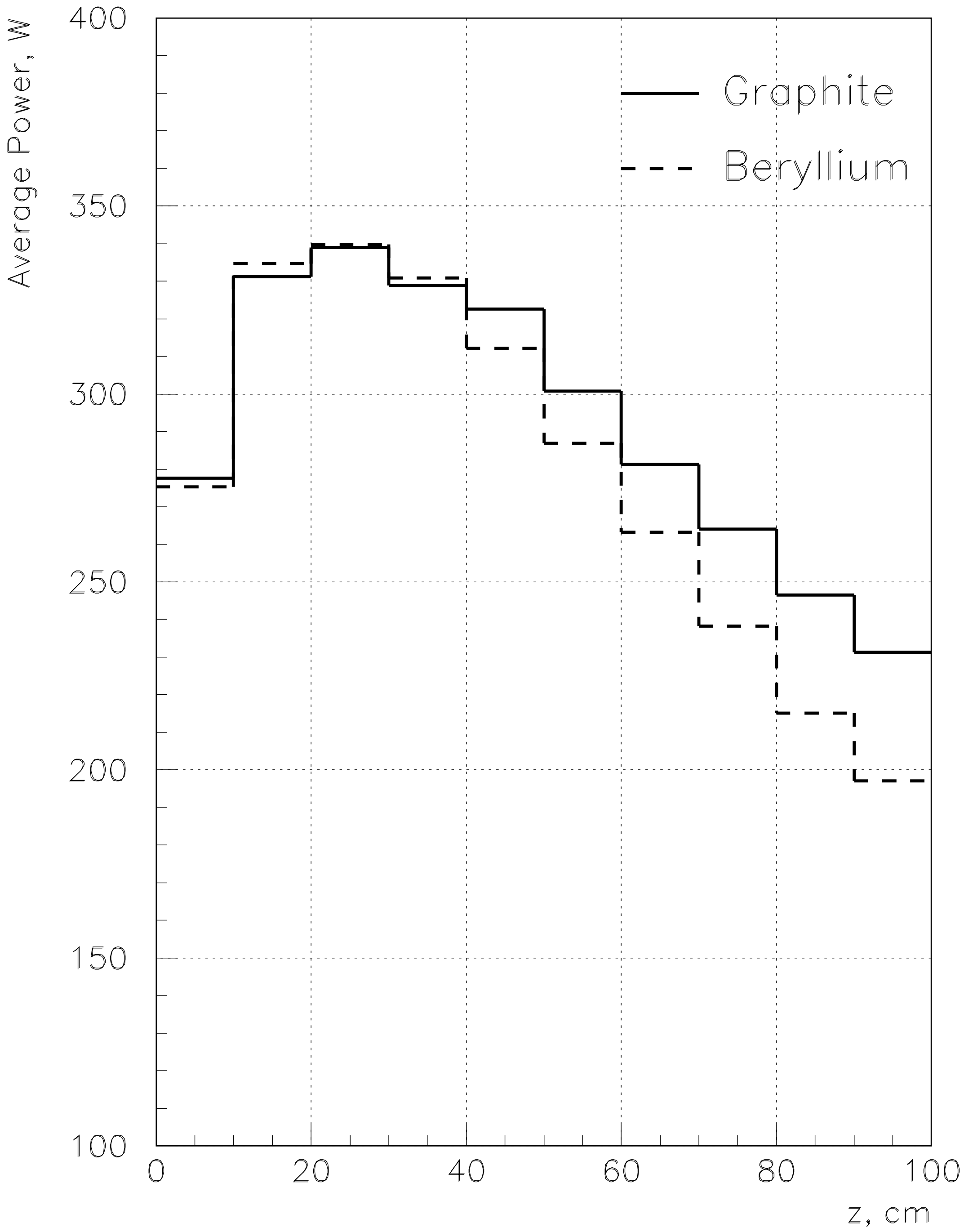

Figure 3.7: Distribution of an average deposited power along the fin target.

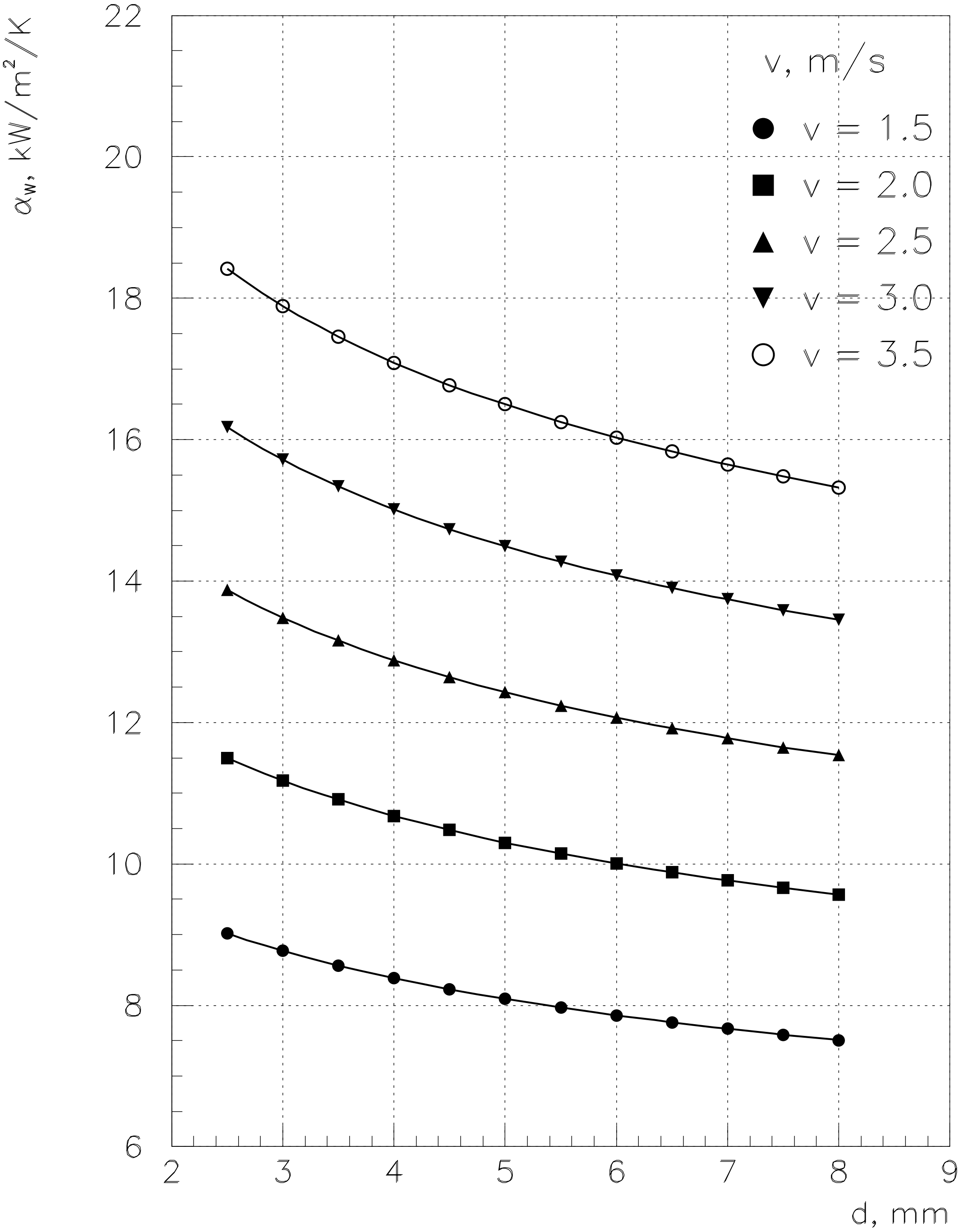

Figure 3.8: Heat transfer coefficient as a function of a pipe diameter and a water flow velocity.

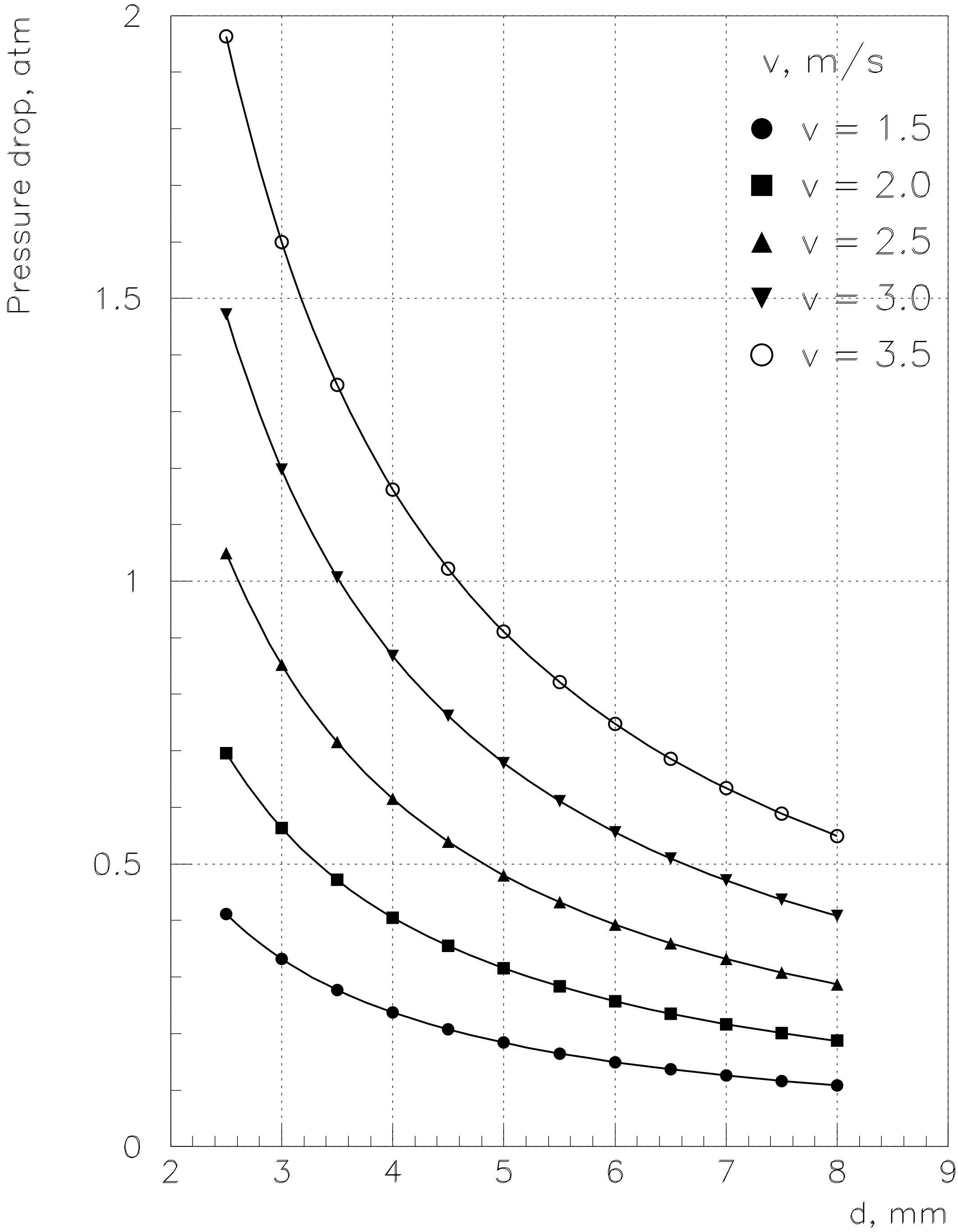

Figure 3.9: Pressure drop for a 1 m length pipe as a function of a pipe diameter and a water flow velocity.

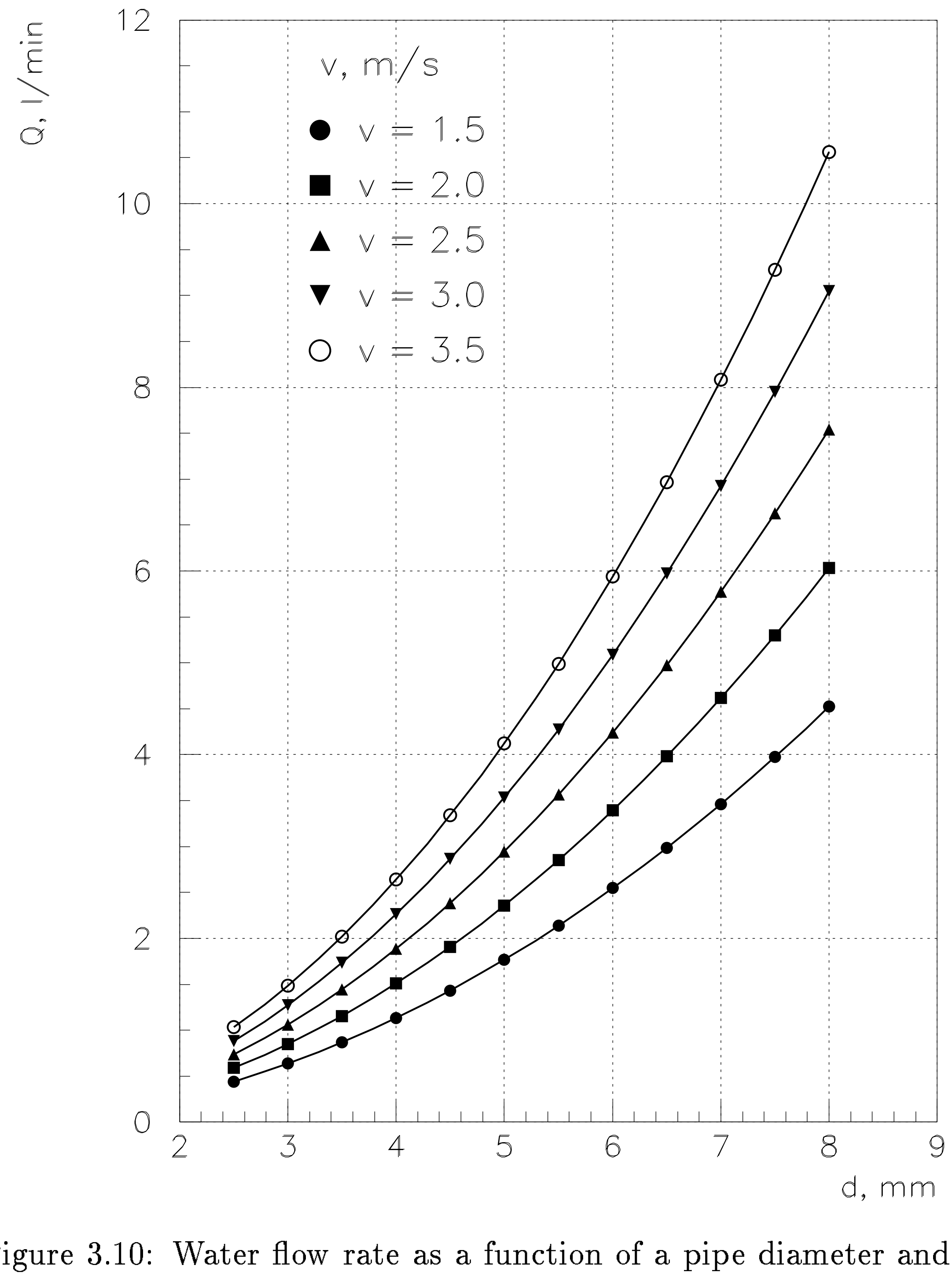

Figure 3.10: Water flow rate as a function of a pipe diameter and a water flow velocity.

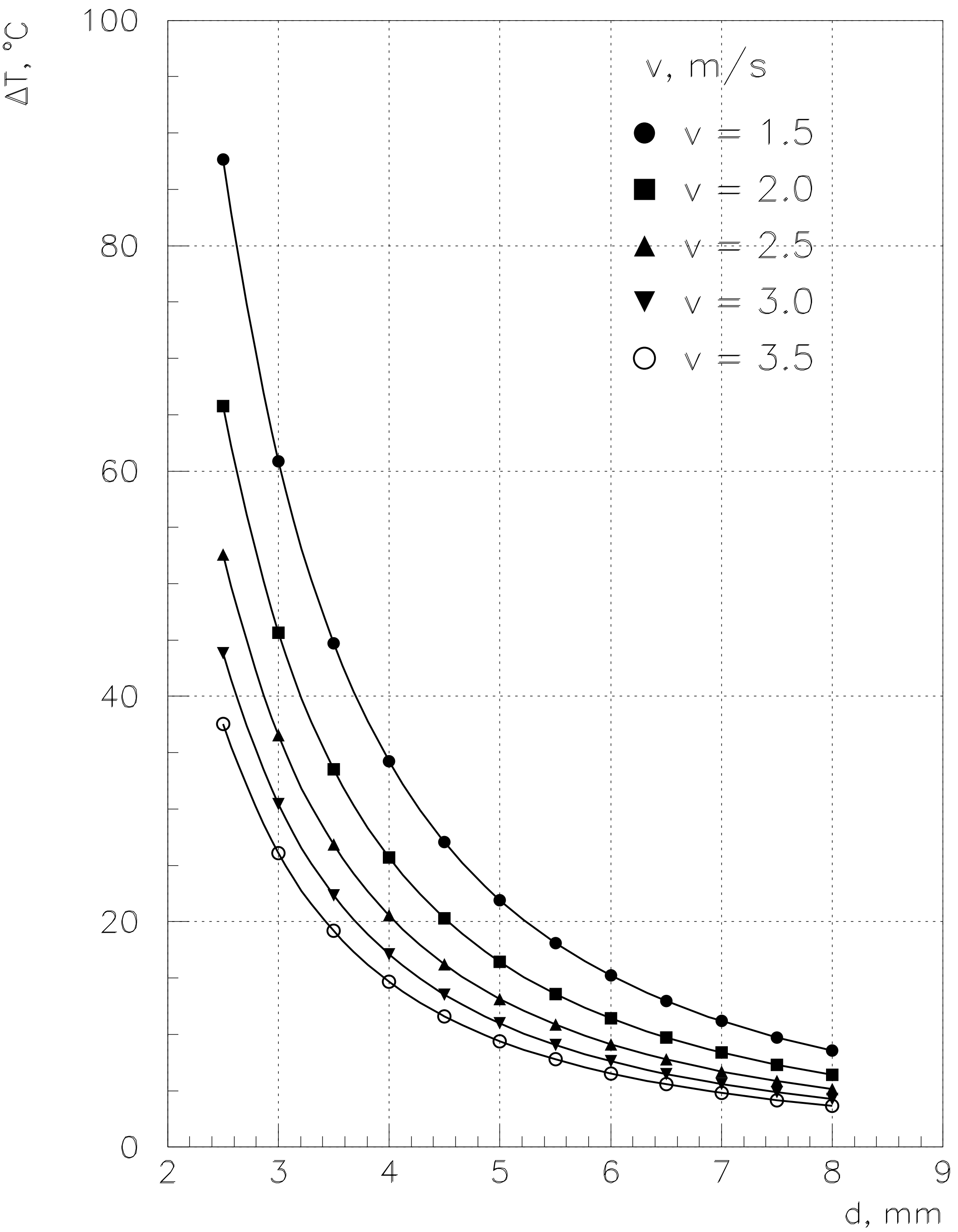

Figure 3.11: Water temperature rise as a function of a pipe diameter and a water flow velocity.

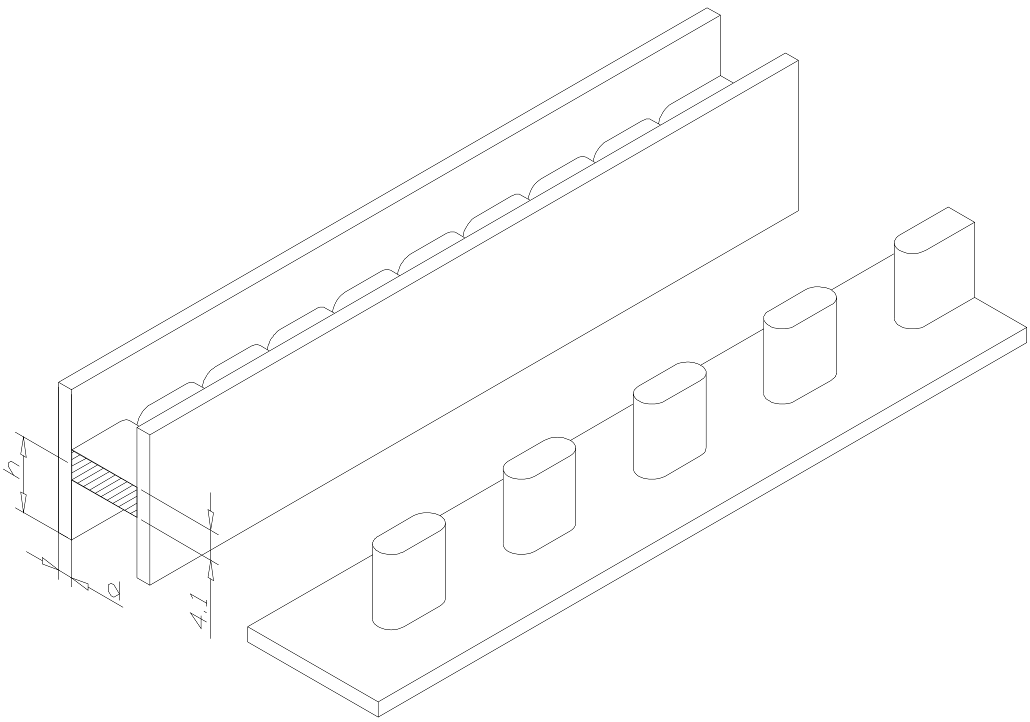

Figure 3.12: Schematical view of the fin target with gas cooling.

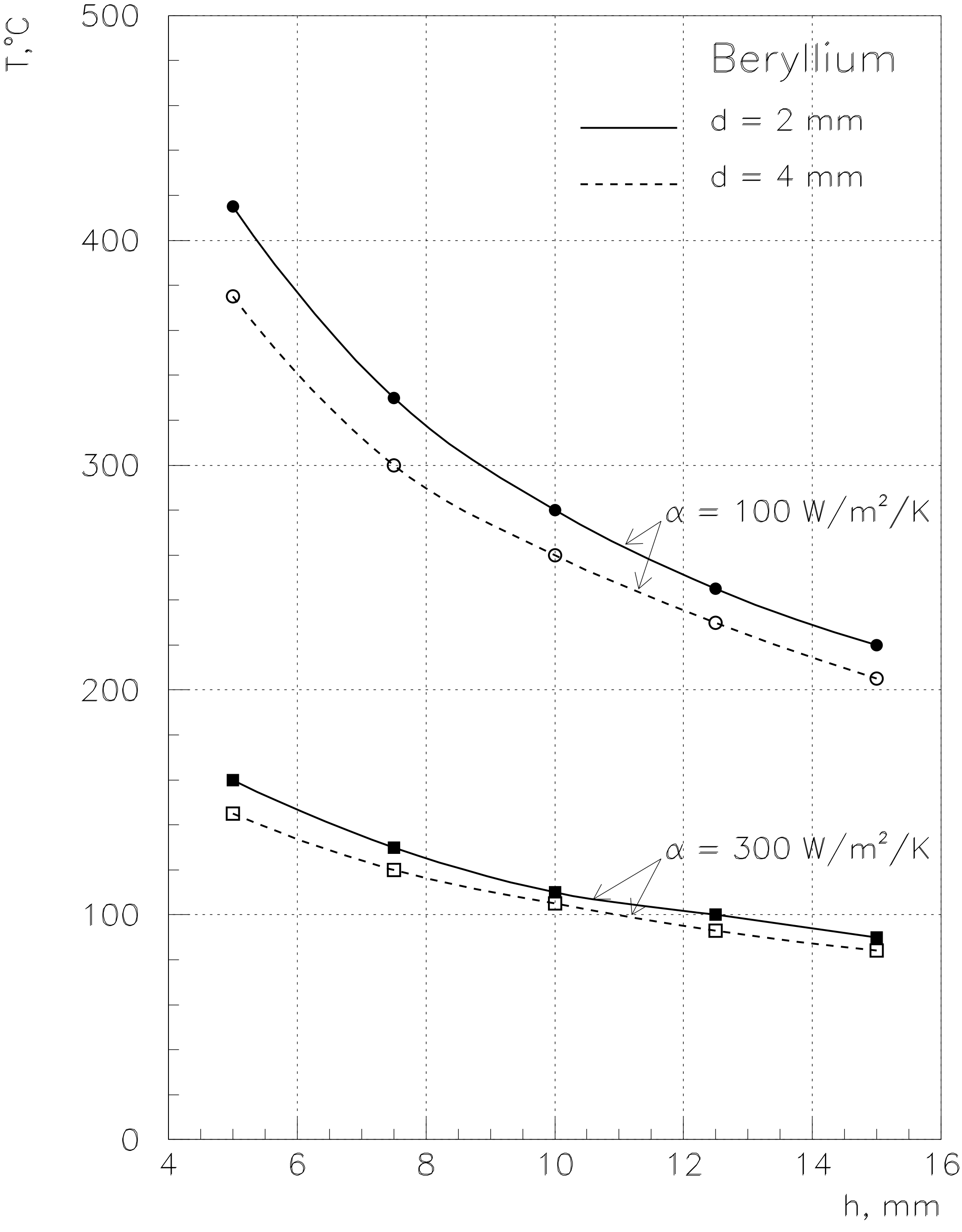

Figure 3.13: Average target temperature as a function of a rib height.

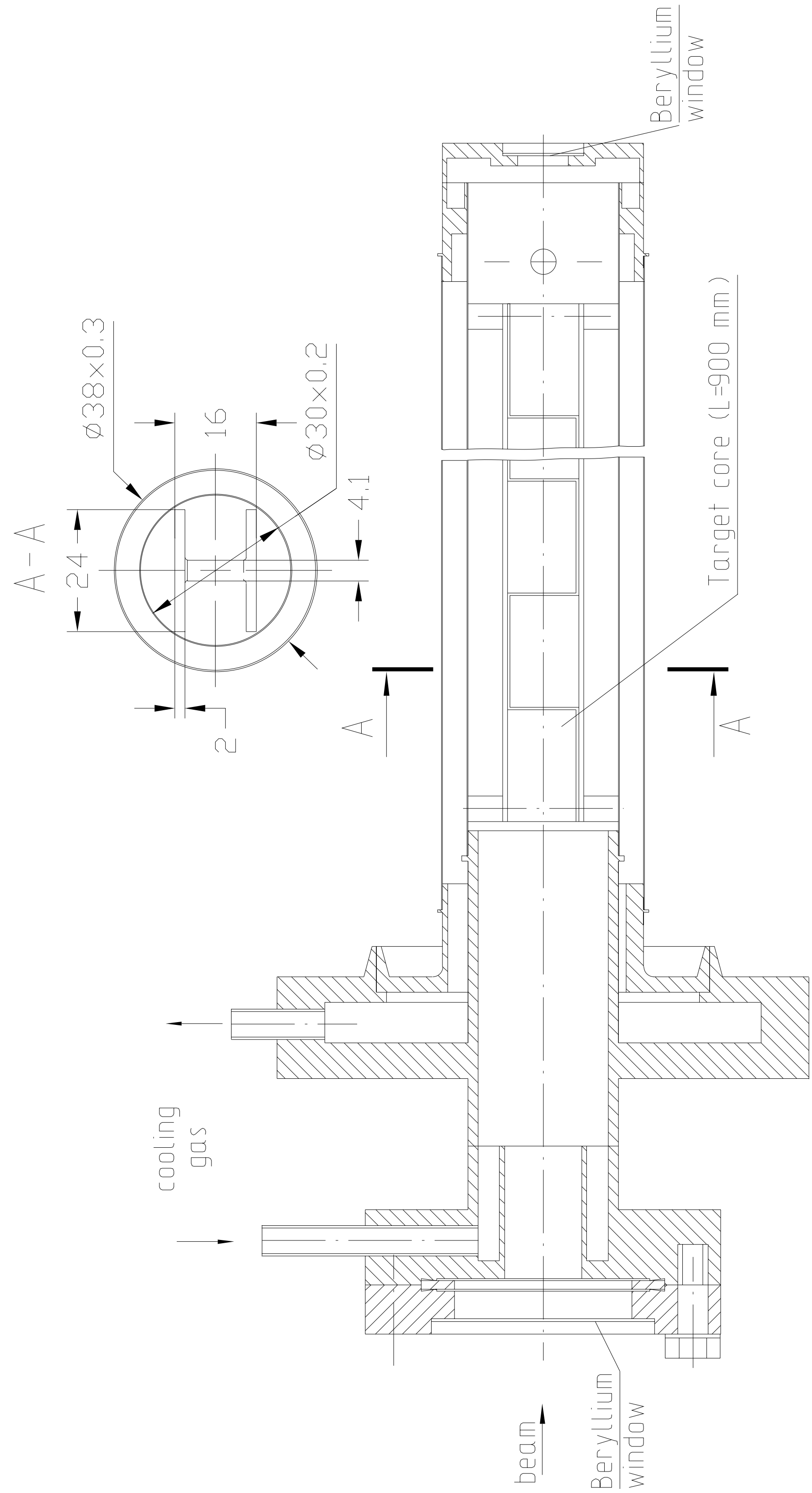

Figure 3.14: Fin target with gas cooling.

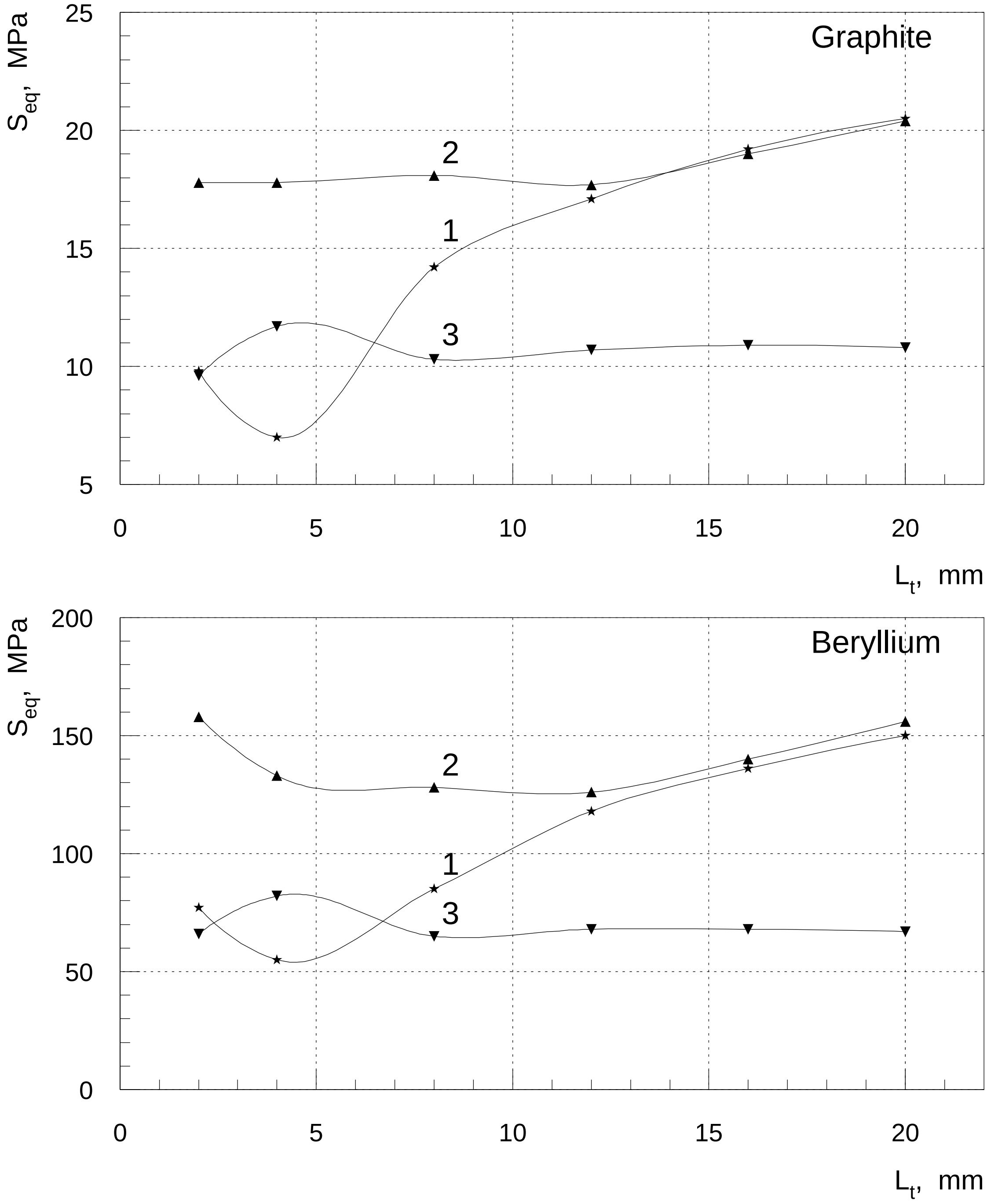

Figure 3.15: Stresses in the gas cooled target as a function of a tooth length.

4 Compensation of the Target Sag

The sag of a target due to its own weight is quite serious problem because the length of a target is significantly higher of its transversal size. Results of the ANSYS analysis for targets described in a previous sections are given in Table 4.1.

Target design	Sag, mm	
	C target	Be target
Water cooled target with a cylindrical core and separate outlet water channel (Figure 2.5)	3.92	2.35
Water cooled target with a cylindrical core and coaxial outlet water channel (Figure 2.6)	3.56	2.48
Gas cooled target with a cylindrical core (Figure 2.10)	0.81	0.61
Fin target with water cooling (Figure 3.6)	0.83	—
Fin target with gas cooling (Figure 3.14)	—	0.33

Table 4.1: Sag of LE targets (ANSYS).

As it follows from Table 4.1 the most serious problem of a target sag is for the LE target design with a water cooled cylindrical core. For the fin target core the sag of 0.6–0.8 mm may be not taken into account because the vertical size of a core and the beam spot size in this direction is significantly larger than the sag.

Different methods of a sag compensations have been verified for the LE target with a water cooled cylindrical graphite core (Figure 2.6). The most simple way of a sag compensation is using of the edge of rigidity, as it is shown in Figure 4.1. This simple method decreases the sag from 3.56 mm to 0.48 mm. But this way may lead to decreasing of a target luminosity due to the beam losses in the edge material.

Another way is the force applied to the downstream end of the target, as it is shown in Figure 4.2. The angle of this force is defined by the Horn sizes and is equal to 1.4°. The force equal to 34 N decreases the maximum sag to 0.23 mm. In the case of two forces (Figure 4.3) the sag may be decreased to 0.045 mm. These forces may be provided by means of strings applied to the points shown in Figure 4.3. More careful analysis of sag compensation should be done at the stage of the advanced conceptual design.

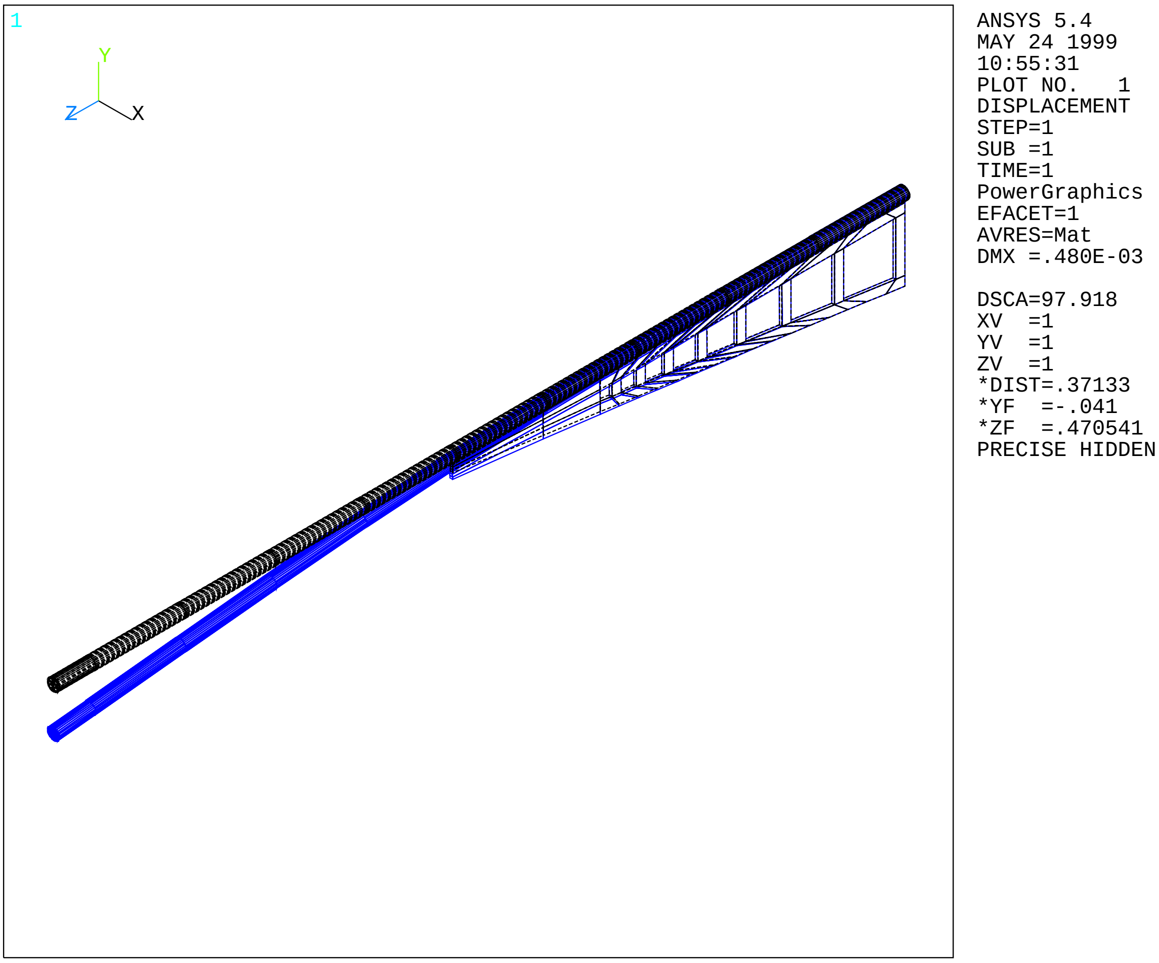

Figure 4.1: Compensation of a target sag by means of an edge of rigidity.

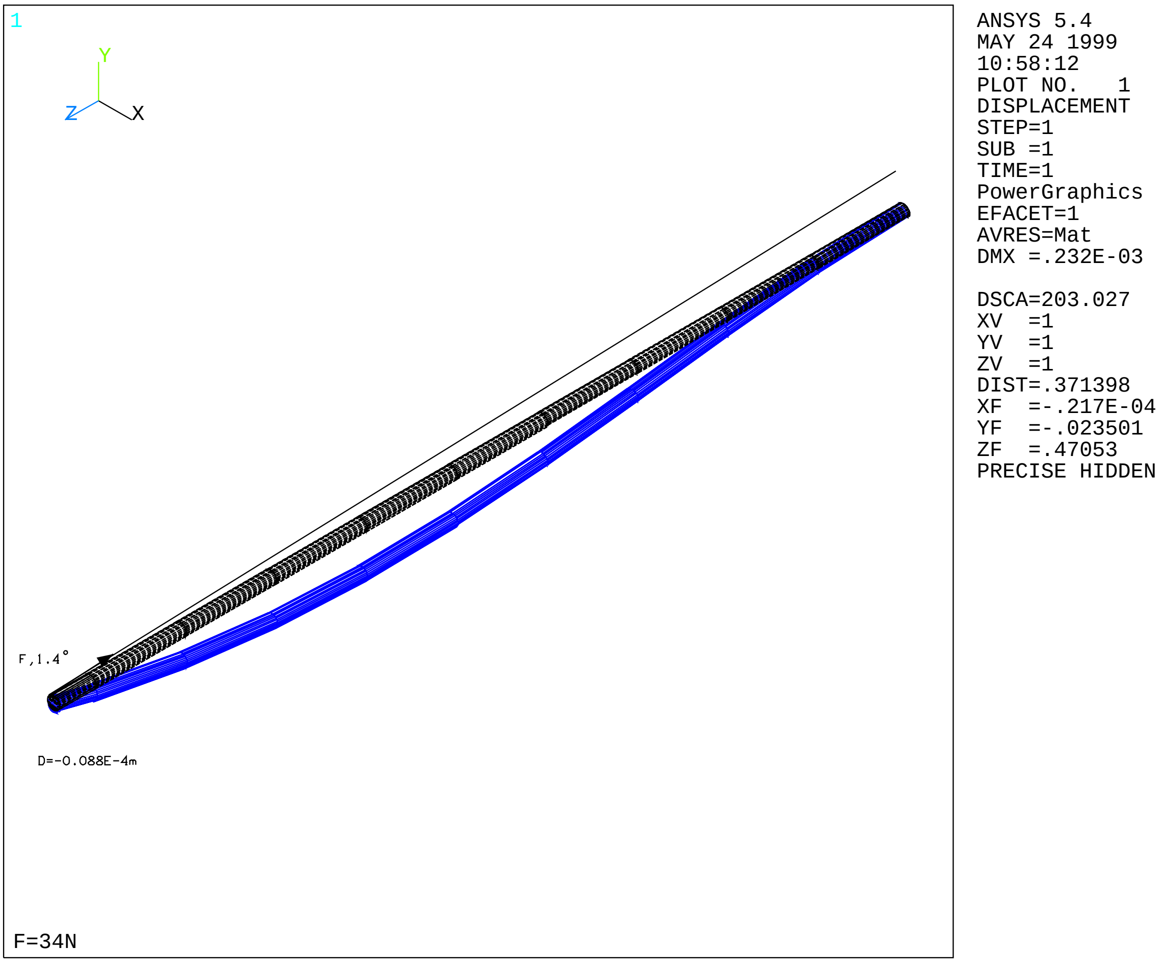

Figure 4.2: Compensation of a target sag by means of a stretched string.

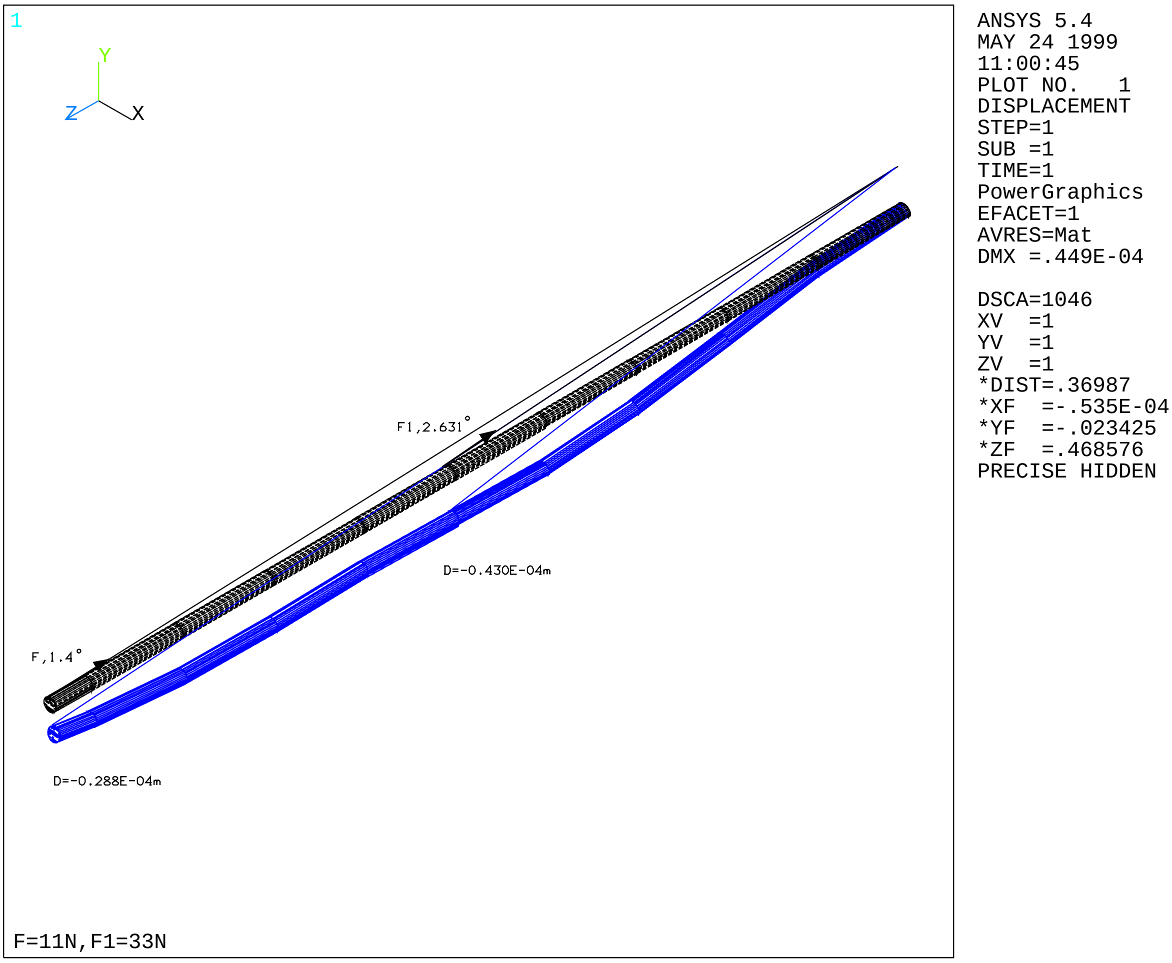

Figure 4.3: Compensation of a target sag by means of two stretched strings.

5 Conclusions

Both possible ways may be applied for cooling of the LE target: water cooling and forced gas convection. In order to decrease a temperature rise of a cooling gas and consequently a target temperature to acceptable levels, the gas cooling system should operate under the static pressure of 1–1.2 MPa. Nitrogen, as well as helium, may be used as a cooling gas.

The average temperature $\overline{T}$ of gas cooled targets is significantly higher than that for water cooled at practically the same values of stresses (see Table 5.1). Higher operating temperatures of target materials correspond to its lower radiation resistance.

	Graphite			Beryllium		
Target design	$\overline{T}$,°C	ΔT,°C	S_{eq}, MPa	$\overline{T}$,°C	ΔT,°C	S_{eq}, MPa
Cyl. core, water cooling	125	345	22.0	50	79	95
Cyl. core, gas cooling	312	264	18.6	300	49	83
Fin core, water cooling	70	282	22.5	70	75	130
Fin core, gas cooling	300	212	20.7	300	56	130

Table 5.1: Temperatures and stresses for various LE target designs.

The analysis of conceptual designs for the LE target, described in previous Sections, allows to make the following conclusions:

- The design with a water cooled cylindrical target core is the most simplest from the point of view of a target construction. It can be easy applied for both considered target materials. The main disadvantage of this design is a rather large sag of the target.

- The water cooled target with a fin core is more complicated in construction with respect to the cylindrical core target because it demands special tooling for brazing of teeth to cooling pipes with accuracy ~0.1 mm at the length of ~900 mm. There are no problems with a sag for fin core targets for both types of cooling.

- In the case of gas cooling, the cylindrical core target is more simple in construction than the fin core target. For both cylindrical and fin target cores graphite is more preferable with respect to beryllium because machining of graphite may be made by usual electrical discharge machine, while beryllium machining demands the special license and special tooling. An erosion of graphite by high velocity gas jet may be prevented by thin film of plasma-sprayed alumina.

Taking into account that targets assumed to be water cooled [3] for the ME and HE beam configurations, two problems of the construction of the water cooled LE target were verified at the stage of its initial conceptual design:

1. The possibility of encapsulating of the graphite target core into stainless steel pipe was verified by means of manufacturing of the ~30 cm sample which corresponds to the downstream part of the target design shown in Figure 2.5. The sample withstood testing by a helium leak detector and shown a good vacuum tightness.

2. Investigations of soldering of a target material and cooling pipes in the water cooled fin target were made for the ZXF–5Q graphite. Two cooling pipes made from the 16X12M2C2 stainless steel (Russian grade widely used in nuclear reactors) were brazed in a vacuum at the temperature ~900°C to graphite plates. Copper-titanium was used as brazing filling material. It was found that for qualitative brazing, the length of the plate should not exceed 30 mm. More long plates undergo the deformation, caused by their stretching due to the difference in coefficients of a thermal expansion of graphite and stainless steel.

The production efficiencies of various LE target designs have been compared using results of GNuMI neutrino beam simulations, which were obtained taking into account main details of each target design. As it follows from these calculations, the difference in neutrino event rates at the far MINOS detector does not exceed 5% for all considered LE target designs and total numbers of ν_μ CC events with $E \leq 6$ GeV are approximately the same as for the 2 mm radius graphite rod (see Figures 1.2 and 1.3).

References

[1] The NuMI Facility Technical Design Report, Fermilab, 1998.

[2] The PH2M Two Horns Focusing System for the NuMI Project, Protvino, 1999, NuMI-B-471.

[3] Advanced Conceptual Design of the Full Scale Fin Target and Engineering Design of the Target Prototypes for the NuMI Project, Protvino, 1998, NuMI-B-454.

[4] Conceptual Design Work and Neutrino Beam Calculations for the NuMI Project, Protvino, 1997, NuMI-B-392.

[5] Status Report: Technical Design of Neutrino Beams for the Main Injector (NuMI), FNAL-TM-1946, NuMI-B-92, Batavia, 1995.

[6] Degtyarev I.I. et al., IHEP Preprint 94-119, Protvino, 1994.

[7] S.P.Timoshenko and J.N.Goodier, Theory of Elasticity, 2nd edition, "Science", Moscow, 1979.

[8] A.Abramov et al, IHEP Preprint 84-64, Serpukhov, 1984.

[9] "Physical Quantities", Handbook, Energoatomizdat, Moscow, 1991.

[10] V.A.Grigoriev, V.M.Zorin, Theoretical Aspects of Heat-technique. Heat-technique Experiment, V.2, Handbook, Energoatomizdat, Moscow, 1988.

[11] The CERN Neutrino Beam to Gran Sasso (NGS), CERN 98-02, Geneva, 1998.

[12] W.Kalbrier, W.C.Middelkoop, P.Sievers, External Targets at the SPS, CERN LABII/BT/74-1, Geneva, 1974.

[13] L.G.Loytzyansky, Mechanics of Liquid and Gas, "Nauka", Moscow, 1970.

[14] J.E.Blocklehurst, Chemistry and Physics of Graphite, V.13, p.205-277.